이학박사학위논문

합성 스캐폴드 단백질을 이용한 MAPK 신호전달의 재구성과 인위적 조작

Reconstruction and artificial manipulation of the MAP kinase signaling cascade using synthetic scaffold proteins

2015년 8월

서울대학교 대학원

생명과학부

류지훈

Reconstruction and artificial manipulation of the MAP kinase signaling cascade using synthetic scaffold proteins

by

Jihoon Ryu

Advisor

Professor Sang-Hyun Park, Ph.D.

A Thesis for the degree of Doctor of Philosophy

June, 2015

School of Biological Sciences

Seoul National University

합성 스캐폴드 단백질을 이용한 MAPK 신호전달의 재구성과 인위적 조작

Reconstruction and artificial manipulation of the MAP kinase signaling cascade using synthetic scaffold proteins

지도교수 박상현

이 논문을 이학 박사 학위논문으로 제출함
2015 년 6 월

서울대학교 대학원
생명과학부
류 지 훈

류지훈의 박사 학위논문을 인준함
2015 년 6 월

위 원 장 허 원기 (인)
부 위 원 장 박 상현 (인)
위 원 김 광윤 (인)
위 원 김 현아 (인)
위 원 최 희정 (인)

Reconstruction and artificial manipulation of the MAP kinase signaling cascade using synthetic scaffold proteins

A dissertation submitted in partial fulfillment

of the requirement for the degree of

DOCTOR of PHILOSOPHY

to the Faculty of

School of Biological Sciences

at

Seoul National University

by

Jihoon Ryu

Date approved

June 30, 2015

Won-Ki Huh

Sang-Hyun Park

Kwang Pyo Kim

Hyun Ah Kim

Hee Jung Choi

ABSTRACT

Reconstruction and artificial manipulation of the MAP kinase signaling cascade using synthetic scaffold proteins

Jihoon Ryu

School of Biological Sciences

Seoul National University

Acting as a hub for eukaryotic cell signaling, scaffold proteins are attractive targets for engineering and manipulating signaling circuits. The ultimate experimental challenge to this premise is to reconstruct a signaling pathway using a rationally designed scaffold with modular architecture. Here, we designed synthetic scaffolds to reorganize the MAPK pathway involved in mating in yeast. The synthetic scaffolds composed of modular interaction domains recruited three member kinases to the plasma membrane and were capable of generating the signaling responses by functioning as logic gates of signaling circuits. The modular architecture of

the synthetic scaffold assembly allowed the artificial manipulation of signaling behaviors, including the modulation of signaling strength and the incorporation of a negative control. Furthermore, this study demonstrated that three tiers of the MAPK pathway exhibited decreasing positional plasticity from the top (MAPKKK) to the bottom (MAPK) tier, suggesting that novel pathway connectivities could be generated. This synthetic approach with designer scaffolds should allow the rational manipulation or engineering of signaling pathways and provide insight into the functional mechanisms of scaffold proteins and scaffold-dependent pathway evolution.

Keywords: MAPK signaling pathway, Synthetic scaffold protein, modular architecture, positional plasticity, scaffold-dependent pathway evolution

Student number: 2006-20413

COPYRIGHT INFORMATION

TABLE OF CONTENTS

LIST OF FIGURES

LIST OF TABLES

ABBREVIATION

DTT	dithiothreitol
EDTA	ethylenediaminetetraacetic acid
EGF	epidermal growth factor
EGFP	enhanced green fluorescent protein
ERK	extracellular signal-regulated kinases
FACS	fluorescence-activated cell sorting
FBS	fetal bovine serum
GST domain	glutathione S-transferase, C-terminal domain
HA	man influenza hemagglutinin
HEPES	4-(2-hydroxyethyl)-1-piperazineethanesulfonic acid
HOG	high osmolarity glycerol
MAPK	mitogen-activated protein kinase
MAPKK	mitogen-activated protein kinase kinase
MAPKKK	mitogen-activated protein kinase kinase kinase
MTD	membrane targeting domain

PKC	protein kinase C
PMSF	phenylmethylsulfonyl fluoride
PSD95	post synaptic density protein
SC media	synthetic complete(SC) media
SDS	sodium dodecyl sulfate
YPD	yeast extract peptone dextrose

INTRODUCTION

Man-made objects often consist of modular parts such as bolts and nuts which are applicable ubiquitously, and those modular parts are assembled into functional units according to rationally designed blueprints. Entities composed of individual modular parts, like a car or a personal computer, could be easily repaired when they malfunction and easily engineered to improve performances or change purposes of the entities via substituting or adding additional modules. If multiple functional modules could be customized and integrated into a single module it would provide an advantage of reducing the size of the entities, but the increased complexity in the architecture of combined modules would compromise the plasticity of the entities and make it difficult to substitute the modules for fixation or improvements. This thesis, to some extent, could be applied to the highly elaborate and complex systems such as living organisms in which correct and precise processing of biological information is crucial for survival.

Using the modular domains of promoters and transcription factors, remarkable advances have been made in the engineering of genetic circuits (*1, 2*). Many studies on designing the information processing circuits have focused on cellular transcription system, mainly due to the modular architecture of the transcriptional machinery. However, in nature, many organisms have also evolved sophisticated cell signaling networks

composed of interlinked signaling proteins in order to glean external and internal information and to decide how to respond to them. Here, we explore the possibility of reorganizing and manipulating a signaling pathway by exploiting modular protein domains.

To test this possibility, we chose scaffold proteins as an engineering target. In many signaling pathways, including the mitogen-activated protein kinase (MAPK) signaling pathways, scaffold proteins have been postulated to function as signaling hubs. These hubs are thought to coordinate signaling by organizing and assembling specific sets of proteins into functional complexes, where signaling information is integrated and processed, thereby generating proper responses (*3*-*7*). As potential organizers directing the flow of information in signaling networks, scaffold proteins are an attractive target for the engineering and manipulation of signaling pathways (*8*-*10*). However, the functional mechanisms and minimal requirements of scaffolds that are critical for engineering and reorganizing a pathway remain unclear (*11*). Different functional domains in native scaffolds often overlap (*12*), and there could be unknown but essential functions in scaffolds yet to be discovered. Although plausible explanations and assumptions for the mechanisms of scaffold functions exist, the complexity and ambiguity of the scaffold functions impede the rational design of a synthetic scaffold protein to rewire a signaling pathway.

In this study, we disrupted the mating MAPK pathway in budding yeast by deleting the native scaffold Ste5 and then attempted to rewire the pathway connectivity using novel designer scaffold proteins composed of modular PDZ interaction domains. The Ste5 scaffold, which is essential for mating signaling, has many functional domains, including docking sites for the signaling proteins of this pathway (*12-18*). However, little is known regarding the minimal requirements for Ste5 function that are necessary for designing synthetic scaffolds to rebuild the mating signaling pathway. We hypothesized that the assembly of protein complexes with a correct membership of component kinases at a specific cellular location would be sufficient for scaffold proteins to activate designated signaling cascades (*19-25*) based on the previously proposed premise that primitive scaffold proteins may have emerged via the combination of simple, yet modular, interactions during the early course of pathway evolution (*26, 27*). By constructing a designer scaffold composed of well-characterized interaction domains to rebuild the signaling connectivity, we explored the wiring principles of MAPK signaling cascades (*28*). Using synthetic designer scaffolds to reconstruct cell signaling pathways helped to circumvents the uncertainty and ambiguity associated with native scaffolds (*29*). Furthermore, the results demonstrate that the modular architecture of the rewired signaling circuit allows the modulation of signaling strength, the incorporation of negative control mechanisms, and the suppression of native

signaling, which suggest the possibility of engineering a novel signaling pathway and artificial manipulation of cell signaling.

RESULTS

The designer synthetic scaffold proteins generated mating responses

We designed synthetic scaffolds composed of various numbers of PDZ domains and a plasma membrane-targeting domain (MTD), which were referred to as PDZ_n^{MTD} (n = 0–7, the number of PDZ domains) (Fig. 1). The second PDZ domain from postsynaptic density protein 95 (PSD95) was used as a building block to recruit three pathway kinases (Ste11, Ste7, and Fus3), and a target peptide (TP) was fused at the C-terminus of the kinases. TPs with an amino acid sequence of -SIESDV can specifically bind to the PDZ domain with moderate affinity (K_d = ~1.3 μM) (*30, 31*). The MTD from Snc2 (*22*) was utilized to localize synthetic scaffolds to the plasma membrane. When expressed in *Δste5* cells, Ste11 (MAP3K), Ste7 (MAP2K), and Fus3 (MAPK) were bound to PDZ_4 in a TP-dependent manner (Fig. 2A), and the PDZ_4^{MTD} complex was localized to the plasma membrane via MTD (Fig. 2B).

To test the ability of synthetic scaffolds to trigger mating signaling, *Δste5* cells containing the genes for PDZ_n^{MTD} and TP-tagged kinases, which were expressed by their own promoters, were stimulated by the heterologous signaling cue of galactose instead of the mating pheromone of α-factor and then monitored for various mating responses. A previous study showed that perturbations of Ste5 assembly caused by replacing Ste11-Ste5

Figure 1.

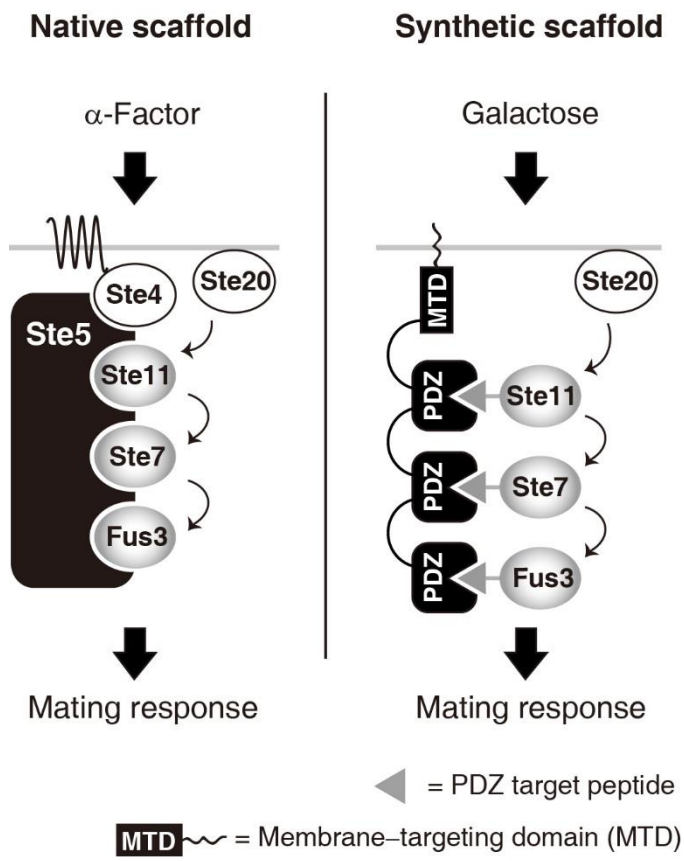
Native scaffold
Synthetic scaffold
α-Factor
Galactose
Ste4
Ste20
Ste5
Ste11
Ste7
Fus3
MTD
PDZ
Mating response
Mating response
= PDZ target peptide
MTD = Membrane–targeting domain (MTD)

Figure 1. Design of the synthetic scaffolds. (Left) Ste5 forms protein complexes with Ste11, Ste7, and Fus3 using distinct binding sites and localizes them to the plasma membrane upon stimulation with mating pheromone (α-factor). (Right) The second PDZ domain of the PSD95 protein was used to recruit Ste11, Ste7, and Fus3 to the synthetic scaffolds, and each kinase was tagged with a TP. The plasma membrane-targeting domain (CTM of Snc2) was used to localize synthetic scaffolds to the plasma membrane. Synthetic scaffold expression was driven by the *gal1* promoter, which was induced by galactose.

Figure 2.

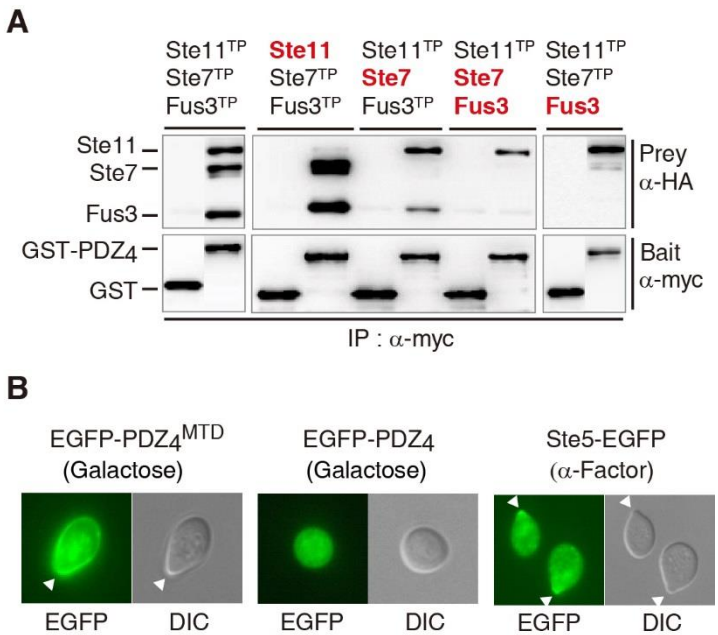
A
Ste11TP Ste7TP Fus3TP
Ste11 Ste7TP Fus3TP
Ste11TP Ste7 Fus3TP
Ste11TP Ste7 Fus3
Ste11TP Ste7TP Fus3
Ste11
Ste7
Fus3
GST-PDZ4
GST
Prey α-HA
Bait α-myc
IP : α-myc
B
EGFP-PDZ4MTD (Galactose)
EGFP-PDZ4 (Galactose)
Ste5-EGFP (α-Factor)
EGFP
DIC
EGFP
DIC
EGFP
DIC

Figure 2. The modular scaffold proteins. (A) IP assays showed that PDZ_4 could bind to Ste11, Ste7, and Fus3 in a TP-dependent manner. Kinases deficient of TP are indicated in red. Myc-tagged GST or GST-PDZ_4 was precipitated with anti-myc antibody-coated agarose beads and detected using anti-myc antibody. The binding of hemagglutinin (HA)-tagged Ste11, Ste7, and Fus3 to GST-PDZ_4 was detected using anti-HA antibody. (B) PDZ_4^{MTD} was recruited to the plasma membrane via the MTD.

or Ste7-Ste5 interactions with heterologous modular domains decreased the mating signaling by two orders of magnitude (*19*). Surprisingly, however, PDZ_n^{MTD} ($n \geq 2$) triggered robust mating responses that were comparable to those by Ste5 as determined by Fus1 transcription (Fig. 3A), Fus3 dual phosphorylation (Fig. 3B), diploid formation (Fig. 4A and Fig. 5B), cell cycle arrest (Fig. 4B), and shmoo formation (Fig. 2B). PDZ_n^{MTD} with increasing numbers of PDZ domains generated corresponding increases in Fus1 transcription (Fig. 3C), suggesting that each PDZ domain is competent for kinase recruitment.

A circuit board for wiring signaling connectivity

As shown in Fig. 2A, the interaction between the PDZ domain and TP determined the assembly of the synthetic scaffold complex. Similarly, PDZ_4^{MTD}-mediated mating signaling was dictated by complex assembly because the mating responses were severely decreased in the absence of TPs on member kinases as determined by Fus3 dual phosphorylation (Fig. 3B), Fus1 transcription (Fig. 5A), and a quantitative mating assay (Fig. 5B). PDZ_4^{MTD}-triggered mating responses were dependent on the membrane-bound kinase Ste20 (Fig. 5C), which phosphorylates Ste11 (*32*). The synthetic scaffold lacking MTD (PDZ_4) led to a dramatic decrease in the mating response, indicating that targeting the synthetic scaffold complex to the plasma membrane is critical for Ste11 activation by Ste20 and thus for

Figure 3.

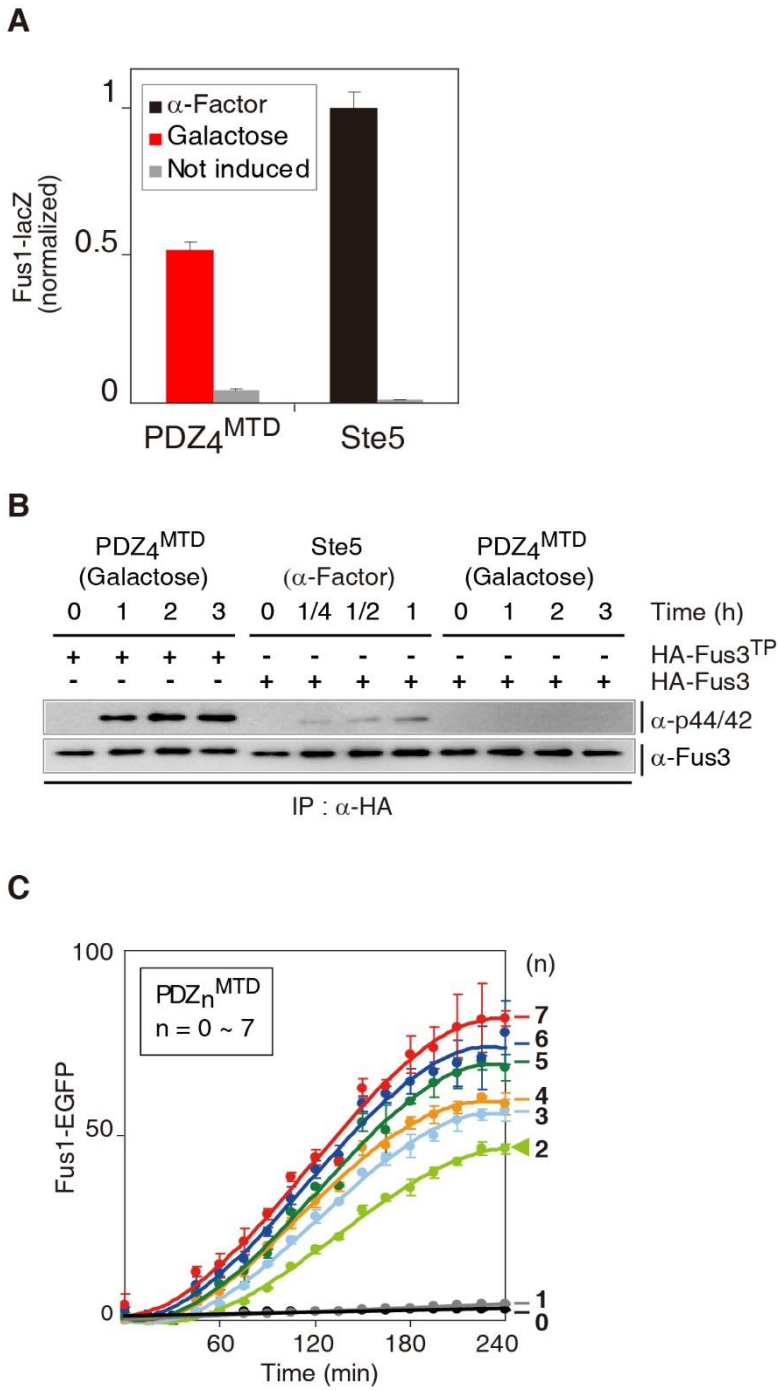
A
α-Factor
Galactose
Not induced
Fus1-lacZ (normalized)
1
0.5
0
PDZ4MTD
Ste5
B
PDZ4MTD (Galactose)
Ste5 (α-Factor)
PDZ4MTD (Galactose)
0 1 2 3 0 1/4 1/2 1 0 1 2 3
Time (h)
HA-Fus3TP
HA-Fus3
α-p44/42
α-Fus3
IP : α-HA
C
PDZnMTD
n = 0 ~ 7
Fus1-EGFP
100
50
0
(n)
7
6
5
4
3
2
1
0
60
120
180
240
Time (min)

Figure 3. Synthetic scaffolds generated mating signaling. (A) Upon stimulation, PDZ_4^{MTD} induced Fus1 transcription as detected by Fus1-lacZ assays. (B) PDZ_4^{MTD} triggered the dual phosphorylation of Fus3 kinase. TP-deficient Fus3 drastically reduced this dual phosphorylation. (C) The mating outputs were monitored by flow cytometry over time using a Fus1- EGFP reporter. Fus1 transcription assays were performed in triplicate. Each of the points represents the mean value ± standard deviation.

Figure 4.

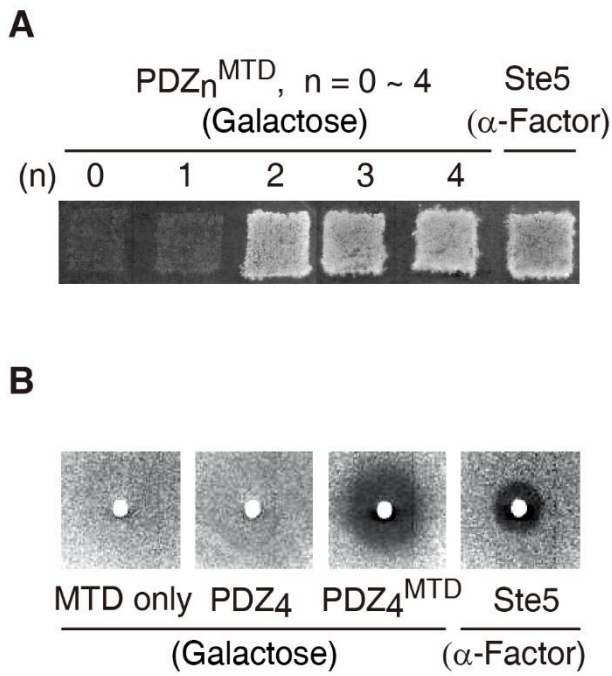
A
PDZn^MTD, n = 0 ~ 4
(Galactose)
Ste5
(α-Factor)
(n) 0 1 2 3 4
B
MTD only
PDZ4
PDZ4^MTD
Ste5
(Galactose)
(α-Factor)

Figure 4. Synthetic scaffolds induced mating responses. (A) PDZ_n^{MTD} ($n \geq 2$) mediated diploid formation as detected by the mating growth assay. (B) Synthetic scaffolds triggered cell cycle arrest at G1 as detected by the halo assay.

Figure 5.

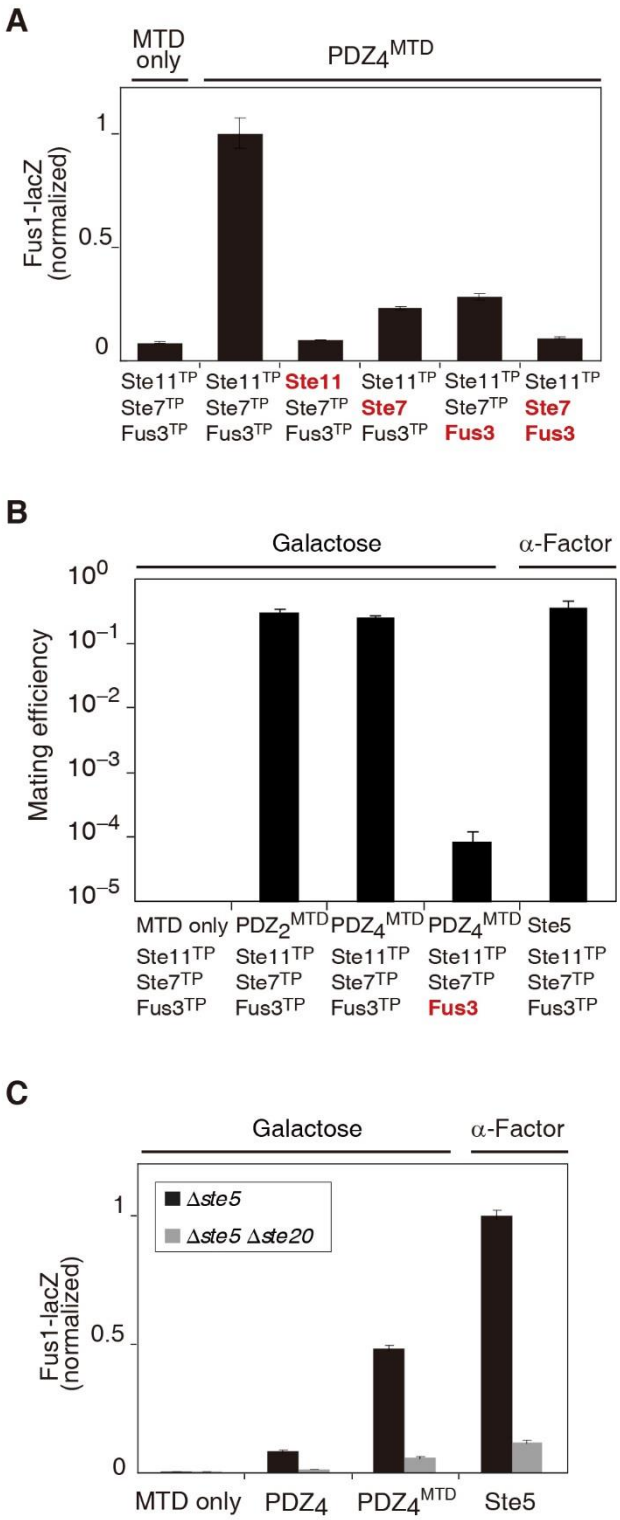
A
MTD only
PDZ4MTD
Fus1-lacZ (normalized)
1
0.5
0
Ste11TP Ste7TP Fus3TP
Ste11TP Ste7TP Fus3TP
Ste11 Ste7TP Fus3TP
Ste11TP Ste7 Fus3TP
Ste11TP Ste7TP Fus3
Ste11TP Ste7 Fus3
B
Galactose
α-Factor
Mating efficiency
10^0
10^−1
10^−2
10^−3
10^−4
10^−5
MTD only
PDZ2MTD
PDZ4MTD
PDZ4MTD
Ste5
Ste11TP Ste7TP Fus3TP
Ste11TP Ste7TP Fus3TP
Ste11TP Ste7TP Fus3TP
Ste11TP Ste7TP Fus3
Ste11TP Ste7TP Fus3TP
C
Galactose
α-Factor
Δste5
Δste5 Δste20
Fus1-lacZ (normalized)
1
0.5
0
MTD only
PDZ4
PDZ4MTD
Ste5

Figure 5. Modular and gate-like characteristics of synthetic scaffold complexes. (A) Interactions between kinases and PDZ_4^{MTD} were critical for activating mating signaling. Perturbations caused by TP removal (in red) dramatically decreased the signaling strength. (B) The quantitative mating assays showed that the mating response was induced by PDZ_4^{MTD}. The mating efficiency decreased dramatically in the absence of the target peptide at Fus3 (in red). The interaction between Ste7 and Fus3 via Fus3 docking sites in Ste7 was not sufficient to provoke the mating response in the synthetic scaffold platform. (C) The rewired signaling by PDZ_4^{MTD} was dependent on membrane-bound Ste20. The Fus1 transcription assays and the quantitative mating assays were performed in triplicate. Each of the points represents the mean value ± standard deviation.

proper signaling (Fig. 5C) as previously reported for Ste5-mediated signaling (*32*). The absence of TP or MTD perturbed the assembly or the membrane-targeting ability of the complex, respectively, and halted signaling. These data suggest that synthetic scaffolds can integrate signaling information, behaving similar to an AND gate in the signaling circuit where the presence of a LOW (0) input signal resulted in a LOW (0) output signal (Fig. 6). In this presentation, the input signals represent the docking interactions of member kinases with PDZ domains (A to C) or the membrane-targeting ability of the scaffold complex (D), and the output signals represent the mating responses (E). The data demonstrate that the simple assembly and plasma membrane-targeting ability of the complex were minimal requirements of the scaffold functions and were sufficient to reconstruct pathway connectivity for generating the mating responses. These findings also suggest that scaffold proteins may have emerged early in evolution and may have functioned to activate signaling via a combination of simple binding affinities for a set of signaling proteins before the emergence of more elaborate control mechanisms (*26*). Interestingly, PDZ_4^{MTD} triggered a higher level of dual phosphorylation of Fus3 than did Ste5 while generating less transcription of the Fus1 gene (Fig. 3A and 3B). This finding is likely due to the attenuated diffusion of activated Fus3 into the nucleus caused by the binding nature of the PDZ domain used in the synthetic scaffolds, as previously predicted in the simple tethering model of scaffold proteins (*33*).

Figure 6.

A

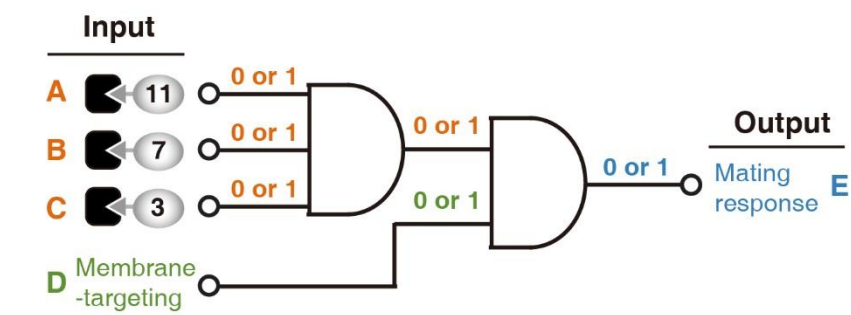

B

Input				Output
A	B	C	D	E
0	0	0	1	0
1	1	1	1	1
0	1	1	1	0
1	0	1	1	0
1	1	0	1	0
1	0	0	1	0
1	1	1	0	0

Figure 6. Schematic diagram for the gate-like behavior of synthetic scaffold complexes. (A) Schematic diagram for the AND gate of the signaling circuit reconstructed by the synthetic scaffolds. The absence or presence of PDZ-kinase docking interactions, membrane-targeting ability of the complex, and mating responses represent 0 or 1, respectively. (B) The truth table for the AND gate tested in this study.

Modular characteristics allow for the artificial manipulation of signaling behaviors

The Ste5 scaffold participates in the negative regulation of mating signaling via modification mechanisms such as phosphorylation by Fus3 (*17*) or G1 cyclin-dependent kinase (*7*). Our synthetic scaffolds, which lack this negative regulatory function by design, were expected to generate a prolonged signaling. Fus1 transcription was monitored using a destabilized GFP reporter carrying a PEST domain (Fus1-EGFP^{PEST}) in *Δste5* cells expressing PDZ$_4^{MTD}$ or Ste5 (*34*). Upon the removal of stimulation, PDZ$_4^{MTD}$ generated a continuous increase in signaling, whereas Ste5 lead to desensitization (Fig. 7). However, the down-regulation of PDZ$_4^{MTD}$-mediated signaling could be achieved via the recruitment of pathway-specific phosphatases such as Msg5 and Ptp3 (*35*) to the scaffold complexes (Fig. 8A). The modular architecture of the synthetic scaffold complex also provided a means to control the magnitude of the signaling output. When TP variants (VKEALV with K_d = 18 μM and VKESLA with K_d = 83 μM) with lower binding affinities (*30*) for the PDZ domain were utilized for Fus3 recruitment, Fus1 transcription and Fus3 dual phosphorylation mediated by PDZ$_4^{MTD}$ were diminished in order of their binding affinities (Fig. 8B and 8C). Together, these results indicate that synthetic scaffolds are amenable to the incorporation of control mechanisms such as negative regulation and to the modulation of signaling strength in an affinity-dependent manner, thus allowing for the reshaping of signaling behaviors. This finding suggests the

Figure 7.

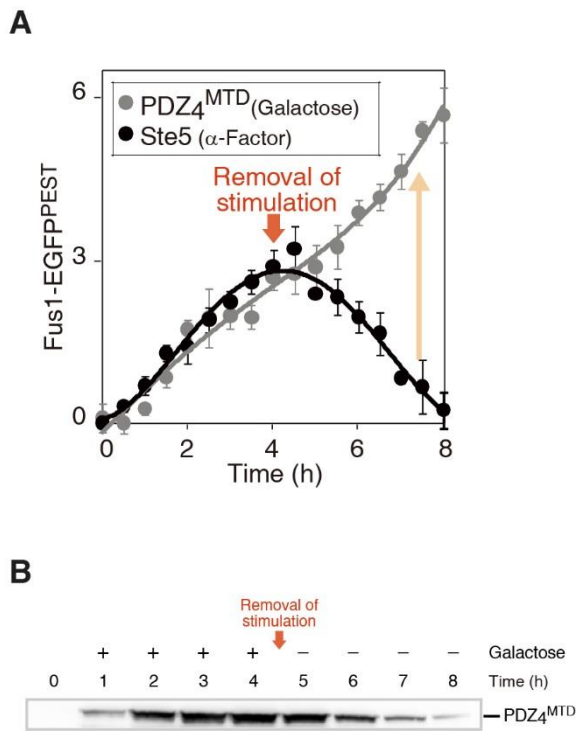
A
PDZ4MTD(Galactose)
Ste5 (α-Factor)
Removal of stimulation
Fus1-EGFPPEST
Time (h)
B
Removal of stimulation
Galactose
Time (h)
PDZ4MTD

Figure 7. Synthetic scaffolds generated a prolonged signaling. (A) The PEST domain of Cln2 from *Saccharomyces cerevisiae* was linked to EGFP to destabilize the protein (*34*). The arrow indicates the time at which the mating pheromone or galactose was removed by changing the media. (B) We have monitored the changes in the quantity of PDZ_4^{MTD} scaffold at varying time points spanning the removal of galactose using western blotting. The expression of synthetic scaffold was induced for 4 hours with media containing galactose prior to changing the media containing glucose. The Fus1 transcription assays were performed in triplicate. Each of the points represents the mean value ± standard deviation.

Figure 8.

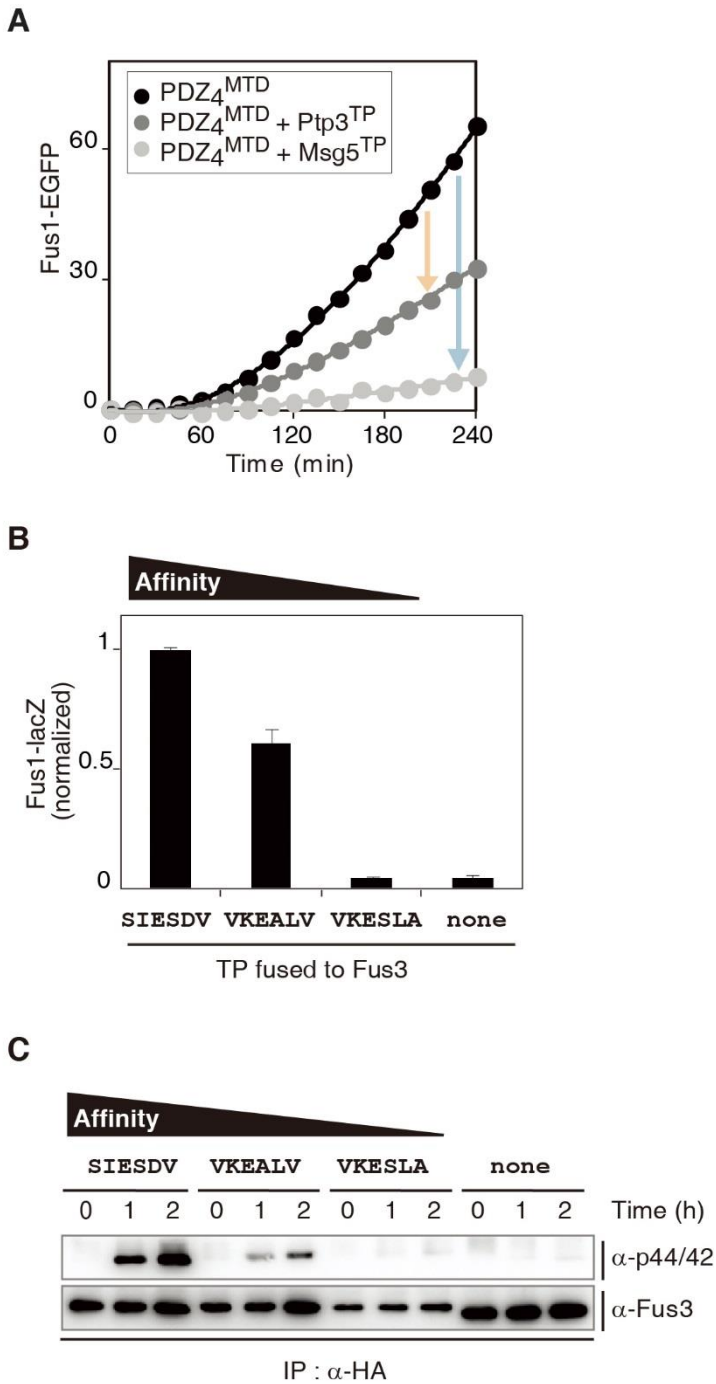
A
PDZ4MTD
PDZ4MTD + Ptp3TP
PDZ4MTD + Msg5TP
Fus1-EGFP
60
30
0
0
60
120
180
240
Time (min)
B
Affinity
Fus1-lacZ (normalized)
1
0.5
0
SIESDV
VKEALV
VKESLA
none
TP fused to Fus3
C
Affinity
SIESDV
VKEALV
VKESLA
none
0 1 2 0 1 2 0 1 2 0 1 2
Time (h)
α-p44/42
α-Fus3
IP : α-HA

Figure 8. Modular characteristics of synthetic scaffolds allow for the artificial manipulation of signaling behavior. (A) PDZ_4^{MTD}-mediated mating responses were suppressed via the recruitment of $Ptp3^{TP}$ and $Msg5^{TP}$ (pathway-specific phosphatases). (B, C) Decreases in the affinity of Fus3 for PDZ_4^{MTD} reduced mating responses. Two target peptides with weaker binding affinities for the PDZ domain than SIESDV were used to recruit Fus3 (*30*). The Fus1 transcription assays were performed in triplicate. Each of the points represents the mean value ± standard deviation.

possibility that various functional domains can be incorporated into modular synthetic scaffolds to materialize elaborate control mechanisms for engineering cell signaling (*10, 36*).

Pathogens often produce scaffold-like proteins to impede or alter the physiology of host cells by wiring a set of host proteins (*33, 37, 38*). For instance, the scaffold protein Vif, which is produced by the human immunodeficiency virus (HIV), targets the antiviral host protein APOBEC3G to a cullin-E2 ubiquitin ligase for degradation (*38*). We tested whether the synthetic scaffold can compete with wild-type Ste5 for TP-tagged member kinases to interfere with the native signaling. The co-expression of PDZ_4, an MTD-deficient synthetic scaffold, in wild-type cells carrying Ste5 dramatically repressed Ste5-mediated signaling output (Fig. 9). The dominant-negative behavior of PDZ_4 may be due to the segregation of member kinases from Ste5. These data imply that engineered scaffold proteins with simple binding affinities for a set of proteins could manipulate host signal transduction and that synthetic scaffold proteins that can intervene in disordered signaling in diseased cells have therapeutic potential.

Positional plasticity in the MAPK signaling circuit

The modular architecture of the synthetic scaffolds provided a means to examine the evolved degree of plasticity of each tier of the MAPK cascade. Ste11, Ste7, or Fus3 kinase in the PDZ_4^{MTD}-mediated complex was

Figure 9.

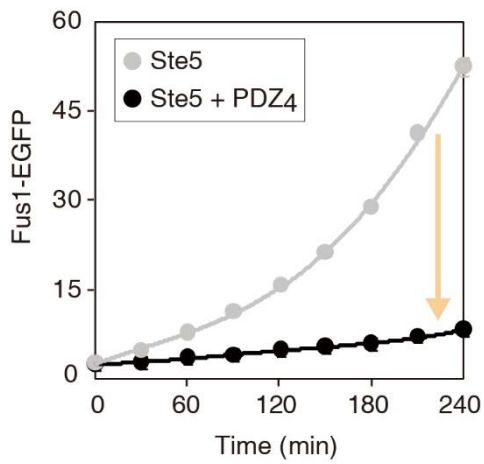

Figure 9. Expression of crippled synthetic scaffold protein (PDZ4) disturbed native mating signaling mediated by Ste5. Ste5-mediated signaling was suppressed by PDZ_4 co-expression in a dominant-negative manner. The Fus1 transcription assays were performed in triplicate. Each of the points represents the mean value ± standard deviation.

replaced one at a time with a kinase from the corresponding tier of non-cognate MAPK pathways such as the high osmolarity glycerol (HOG) and protein kinase C (PKC) pathways in yeast cells (Fig. 10A). The tolerance of each tier to non-cognate pathway members was monitored by measuring the output from pathways that were composed of mixed sets of kinases assembled by PDZ_4^{MTD} (Fig. 10B and 10C). The top tier of the mating cascade was highly tolerant to non-cognate kinases, particularly Ssk22 from the HOG pathway. Ssk22 transmitted signals through Ste7 and Fus3 and generated a robust output that was comparable to ~75% of that by Ste11 (Fig. 11A and 12A). The middle tier was somewhat tolerant to Mkk1 from the PKC pathway, whereas the bottom tier was not tolerant to any of the tested kinases (Fig. 11B, 11C, 12B, and 12C). This result indicates that the positional plasticity of the three tiers of MAPK cascades has been manifested in the order of MAP3K > MAP2K > MAPK in the synthetic scaffold platform. This finding is reminiscent of cell signaling requirements, such as the demands for accommodating multiple upstream inputs at the upper tiers of pathways and for dictating signaling specificity by a terminal kinase. It was previously reported that the interaction between Ste7 and Fus3 through docking sites in Ste7 is essential for the recruitment of Fus3 to the Ste5 complex and thus for proper signaling (*17*). To test this issue in the context of synthetic scaffold-mediated signaling, we used a Ste7 variant, Ste7(ND), in which two Fus3-docking sites were mutated (*39*). $Ste7(ND)^{TP}$ decreased the magnitude of PDZ_4^{MTD}-mediated Fus1 transcription to a basal

Figure 10.

A

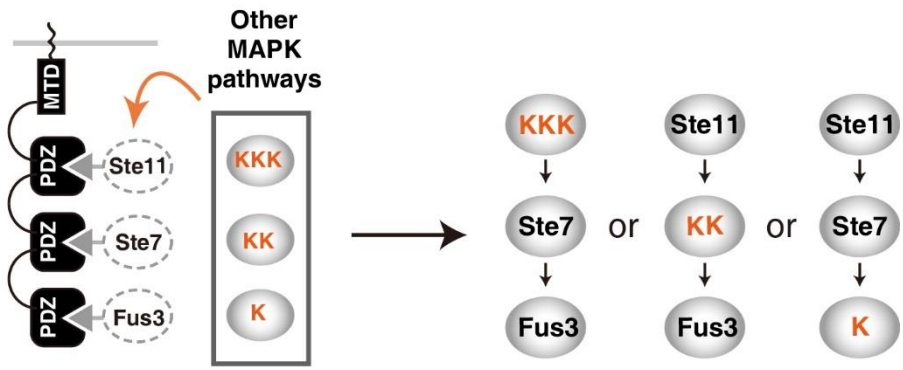

B

	Mating pathway		Osmoregulatory pathway		Protein kinase C pathway	
MAP3K	Ste11	+ + +	Ssk22	+ +	Bck1	+
MAP2K	Ste7	+ + +	Pbs2-kinase domain	–	Mkk1/ Mkk2	+ / –
MAPK	Fus3	+ + +	Hog1	n.d.(–)	Slt2	n.d.(–)

C

Kinase tested	Relative signaling strength
Ssk22	74% (++)
Bck1	14% (+)
Mkk1/Mkk2	19% (+) / 11%(–)
Pbs2-kinase domain	12%(–)
Hog1	n.d.(–)
Slt2	n.d.(–)

Figure 10. Positional plasticity of the three tiers of the mating MAPK pathway. (A) Pathway plasticity was determined by measuring the tolerance of the rewired mating pathway to non-cognate components from other MAPK pathways in yeast. (B) Components in the mating MAPK pathway were replaced with non-cognate members from the HOG or PKC pathways. The symbols (+++), (++) and (+) indicate 100%, 50–100% and 10–50% of synthetic scaffold-mediated signaling strength with a wild-type set of kinases, respectively. n.d. means “not detected”. (C) Detailed value of relative signaling strength.

Figure 11.

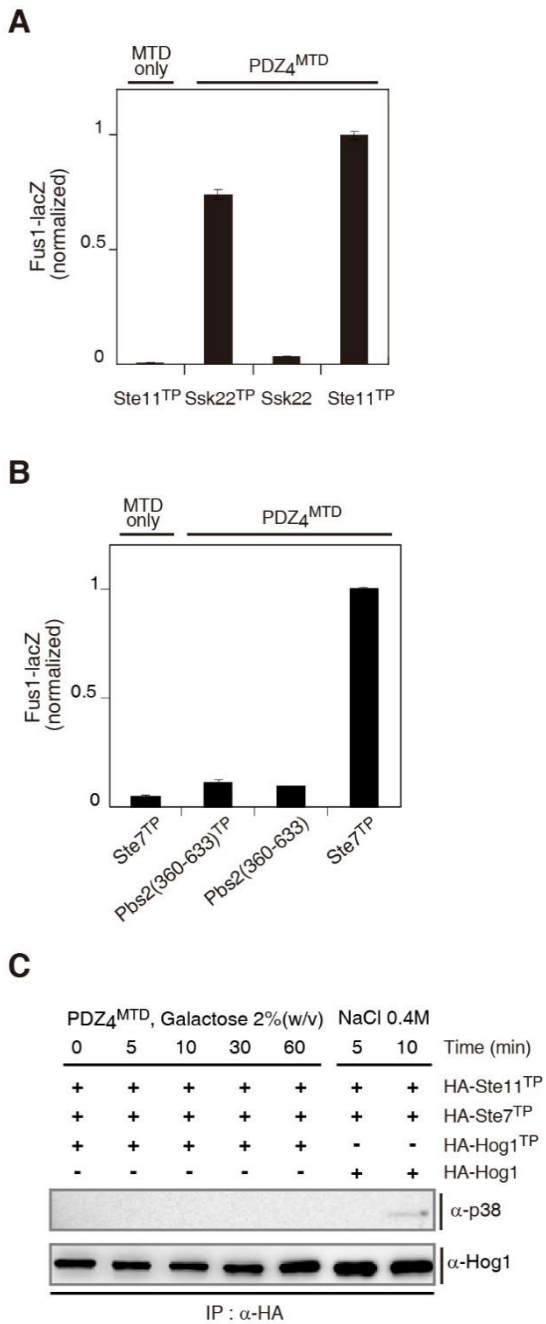
A
MTD only
PDZ4MTD
Fus1-lacZ (normalized)
1
0.5
0
Ste11TP
Ssk22TP
Ssk22
Ste11TP
B
MTD only
PDZ4MTD
Fus1-lacZ (normalized)
1
0.5
0
Ste7TP
Pbs2(360-633)TP
Pbs2(360-633)
Ste7TP
C
PDZ4MTD, Galactose 2%(w/v)
NaCl 0.4M
0 5 10 30 60 5 10 Time (min)
+ + + + + + + HA-Ste11TP
+ + + + + + + HA-Ste7TP
+ + + + + - - HA-Hog1TP
- - - - - + + HA-Hog1
α-p38
α-Hog1
IP : α-HA

Figure 11. The tolerance of each tier of the mating MAPK pathway to the high osmolarity glycerol (HOG) pathway members. (A) In place of Ste11, Ssk22 transmitted signaling through the mating MAPK pathway. (B) Ste7 in the PDZ_4^{MTD}-mediated complex was replaced with Pbs2(360–633). Pbs2(360–633) did not transmit signaling through the signaling complex. (C) Fus3 in the PDZ_4^{MTD}-mediated complex was replaced with Hog1. Hog1 was not activated by Ste7. Fus1 transcription assays were performed in triplicate. Each of the points represents the mean value ± standard deviation.

Figure 12.

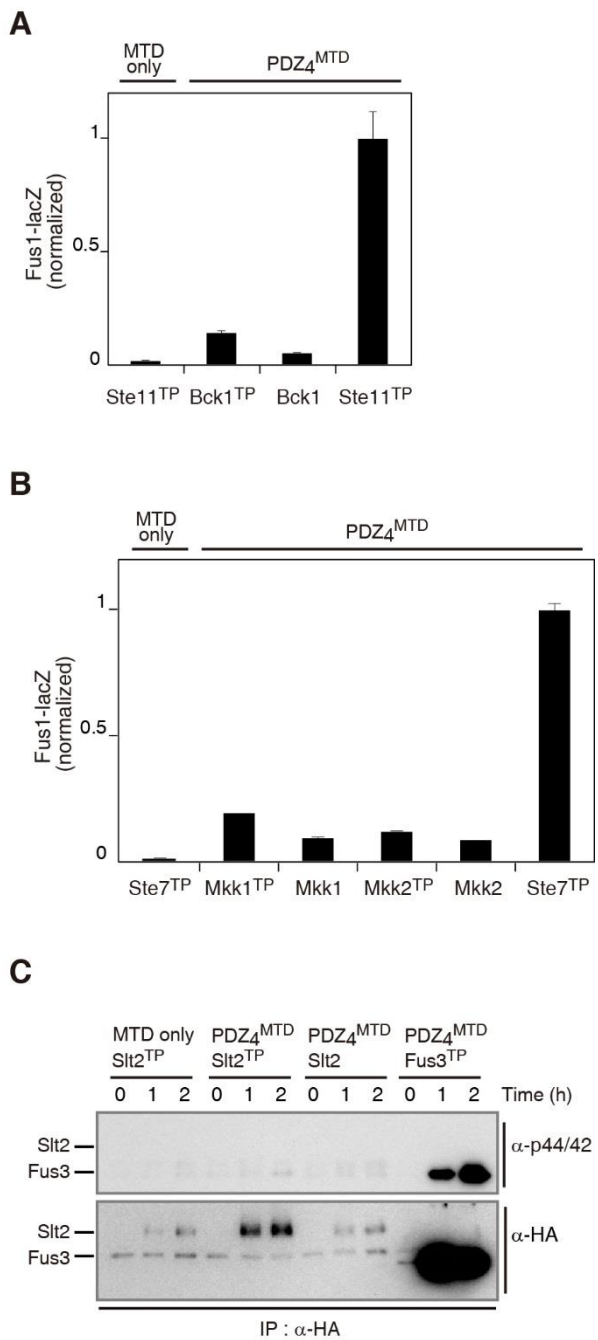
A
MTD only
PDZ4MTD
Fus1-lacZ (normalized)
1
0.5
0
Ste11TP
Bck1TP
Bck1
Ste11TP
B
MTD only
PDZ4MTD
Fus1-lacZ (normalized)
1
0.5
0
Ste7TP
Mkk1TP
Mkk1
Mkk2TP
Mkk2
Ste7TP
C
MTD only Slt2TP
PDZ4MTD Slt2TP
PDZ4MTD Slt2
PDZ4MTD Fus3TP
0 1 2 0 1 2 0 1 2 0 1 2 Time (h)
Slt2
Fus3
α-p44/42
Slt2
Fus3
α-HA
IP : α-HA

Figure 12. The tolerance of each tier of the mating MAPK pathway to the protein kinase C (PKC) pathway members. (A) In place of Ste11, Bck1 transmitted signaling through the mating MAPK pathway. (B) Ste7 in the PDZ_4^{MTD}-mediated complex was replaced with Mkk1 or Mkk2. Mkk1 transmitted signaling through the mating MAPK pathway. (C) Fus3 in the PDZ_4^{MTD}-mediated complex was replaced with Slt2. Slt2 was not activated by Ste7. Fus1 transcription assays were performed in triplicate. Each of the points represents the mean value ± standard deviation.

level (Fig. 13). Surprisingly, Ste7-Fus3 docking remained critical for signaling by the synthetic scaffold assembly, in which Fus3 was independently recruited to the complex via PDZ-TP interaction. This finding suggests that docking interactions between Ste7 and Fus3 may play critical roles in the activation of Fus3 in addition to the recruitment of Fus3 to the scaffold complex, for example, by ensuring the correct projection of bound Fus3 for proper catalysis, which is also consistent with decreases in plasticity at the lower tiers of the MAPK pathway (Fig. 10B and 10C). Together, these data imply that the manipulation of interaction domains in signaling proteins may be critical in the construction of non-natural signaling pathways by recombination or artificial engineering, particularly at the lower tiers of pathways.

Unique behaviors of the synthetic scaffolds

One of the intriguing findings in this study was that the synthetic scaffold carrying two PDZ domains (PDZ_2^{MTD}) could generate a substantial magnitude of signaling output from a three-tiered kinase cascade (Fig. 3C, 4A, and Fig. 5B). One of plausible models for explaining this is the non-static assembly of the PDZ_2^{MTD}-mediated complex, in which the bound kinases are dynamically exchanged. For example, Ste11 is released from PDZ_2^{MTD} after activating Ste7, and then Fus3 occupies the empty docking site followed by activation by Ste7 (Fig. 14A). This explanation seems

Figure 13.

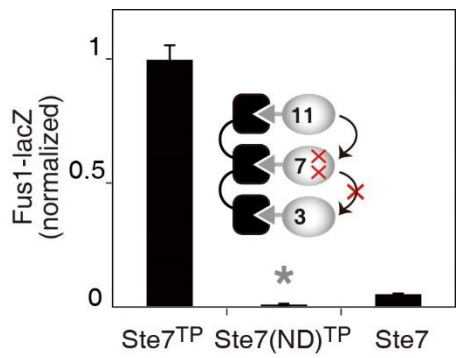

Figure 13. Interaction between MAP2K and MAPK via docking sites in MAPK contributes to signaling specificity. Both Fus3 docking sites (*39*) and the TP of $Ste7^{TP}$ were required to induce synthetic scaffold-mediated signaling. Fus1 transcription assays were performed in triplicate. Each of the points represents the mean value ± standard deviation.

Figure 14.

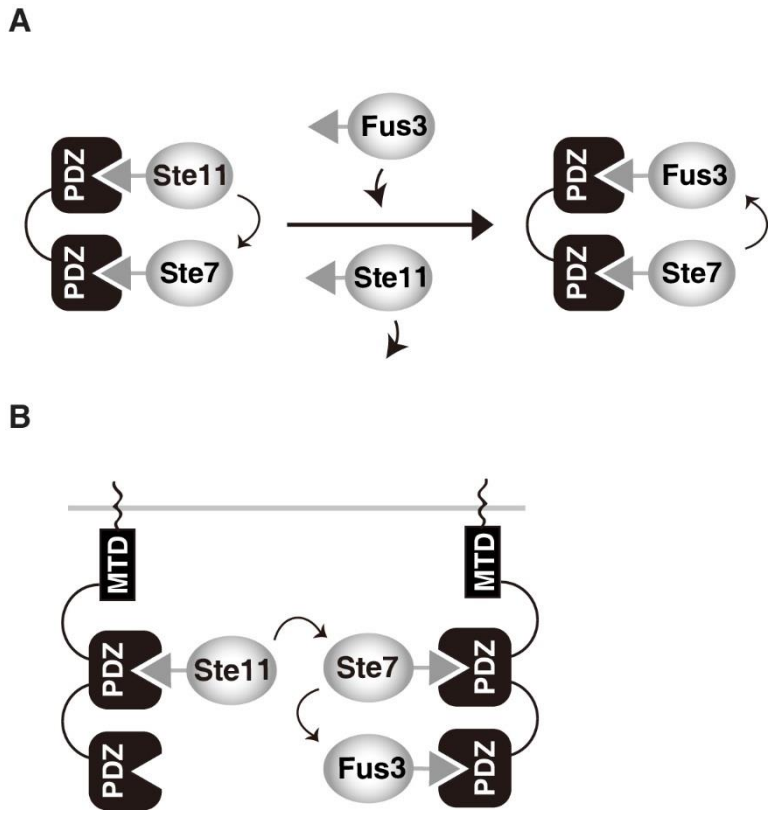
A
Fus3
PDZ
Ste11
PDZ
Ste7
Ste11
PDZ
Fus3
PDZ
Ste7
B
MTD
MTD
PDZ
Ste11
Ste7
PDZ
PDZ
Fus3
PDZ

Figure 14. Plausible models for the activation of the three-tiered cascade of the mating MAP kinase pathway by PDZ_2^{MTD} in yeast. (A) A plausible mechanism by which the synthetic scaffold with two PDZ domains mediates three-tiered kinase cascades is shown. (B) PDZ_2^{MTD} may cluster at the plasma membrane to induce the cross-activation of kinases in different scaffold complexes.

consistent with the fairly fast k_{off} rate (15 s^{-1}) of the PDZ-TP interaction (*31*). Another possibility is that PDZ_2^{MTD} scaffolds charged with different combinations of kinases cluster at the plasma membrane. The elevated local concentration of the scaffold complexes may lead to the cross-activation of kinases (Fig. 14B) (*40*). This finding implies that all three member kinases may not necessarily be bound simultaneously to the scaffold for the activation of signaling.

Another interesting point is that a similar synthetic scaffold was able to rewire the ERK/MAPK pathway in mammals (Fig. 15), showing that the synthetic approach used in this study is not limited to yeast signaling and is potentially applicable to higher organisms. Upon stimulation by EGF, the synthetic scaffold generated sustained dual phosphorylation of ERK in 293T cells. The result suggests that the rewiring of signaling pathways by artificial assembly of scaffold complex could be ubiquitously applicable to higher eukaryotes.

Figure 15.

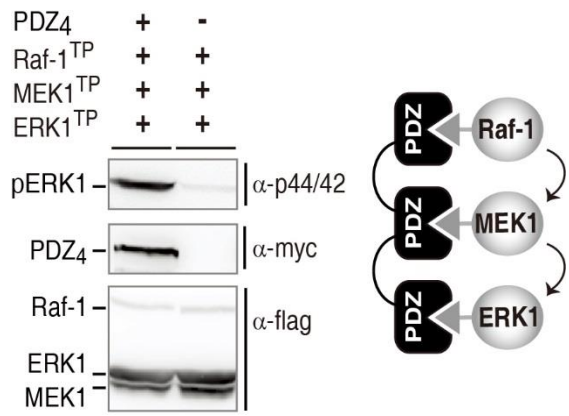
PDZ4 + -
Raf-1TP + +
MEK1TP + +
ERK1TP + +
pERK1
α-p44/42
PDZ4
α-myc
Raf-1
ERK1
MEK1
α-flag
PDZ
Raf-1
PDZ
MEK1
PDZ
ERK1

Figure 15. This design principle could be applicable to other organisms. Upon EGF (100 ng/mL) stimulation for 1 hour, the PDZ-based synthetic scaffold protein mediated ERK dual phosphorylation. Raf-1 (MAP3K), MEK1 (MAP2K), and ERK1 (MAPK) were tagged with TP.

DISCUSSION

Simple scaffolds carrying only the binding affinities for member kinases of a signaling pathway have been the popular subject of several theoretical modeling studies (*33, 40, 41*). Lowering the entropic barrier to intracellular protein-protein interactions by simple binding scaffolds has been proposed to be an effective means to enhance the production of valuable metabolites in metabolic engineering (*21*) or in signaling engineering in prokaryotic cells (*42*). However, this premise has not been experimentally tested in signaling networks in eukaryotic cells. Furthermore, various reports have suggested that some scaffolds can actively elicit the interaction-mediated activation of signaling proteins to facilitate signal transduction (*17, 18, 43, 44*).

In this study, we designed synthetic scaffold proteins with well-characterized interaction domains, including PDZ and MTD, to rewire the mating MAPK signaling pathway in yeast. Cells carrying the synthetic scaffold proteins responded to the heterologous cue of galactose and generated the mating MAPK signaling responses in the absence of the native scaffold, Ste5. By rationally designing the scaffold proteins from scratch, we could determine the minimal requirements of scaffold functions. The results demonstrated that the assembly of the correct set of component kinases and targeting of the complex to the plasma membrane were

sufficient for wiring the pathway connectivity and for generating the pathway outputs. Furthermore, our results indicate that the three-dimensional arrangements of signaling proteins complexed with a scaffold protein may not be critical, at least, for the onset of signaling because the PDZ domains used in the synthetic scaffolds were linked using a flexible peptide linker and presumably shared little structural similarity with the native scaffold.

There have been wide speculations on *how* the scaffold proteins have emerged during the evolution of cell signaling network. One of the proposed models is that primitive scaffolds may have emerged via the combination of modular interactions during the early course of pathway evolution (*26, 27*). On the other hand, little is known about *why* scaffolds have emerged during the pathway evolution. Harris *et al*. (*23*) previously demonstrated that covalently linked member kinases of the mating pathway can activate the mating signaling in the absence of the native scaffold, Ste5. This suggests two possible routes to materialize pathway specificity and connectivity during the evolution of signaling pathways. One is to wire member kinases via scaffold-dependent non-covalent assembly and the other is covalent linking of member kinases (Fig. 16). We know for a fact that nature took the former route. Why the signaling network has evolved to employ scaffold-dependent assembly instead of covalent linking of kinases? Our study provides implications on the possible advantages of the scaffold-dependent

Figure 16.

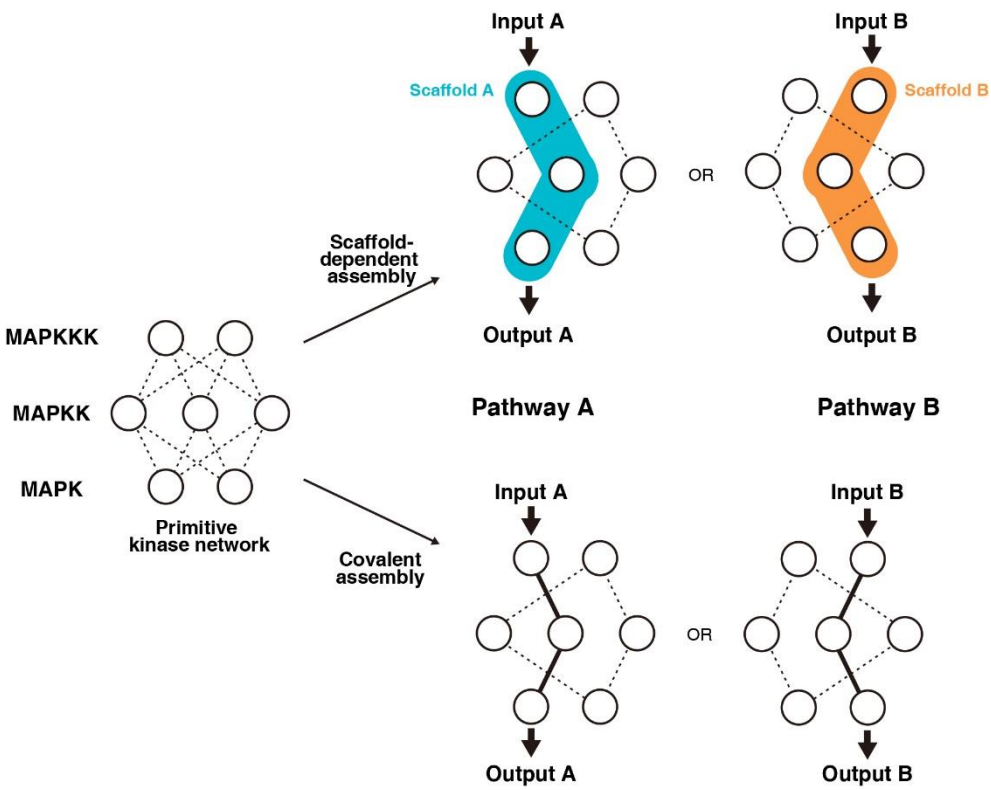
Input A
Scaffold A
OR
Input B
Scaffold B
Scaffold-
dependent
assembly
Output A
Output B
MAPKKK
MAPKK
MAPK
Pathway A
Pathway B
Primitive
kinase network
Covalent
assembly
Input A
OR
Input B
Output A
Output B

Figure 16. Two possible routes to generate specific MAPK signaling pathways from a primitive kinase network. Many organisms have evolved scaffold-dependent assembly of signaling complexes instead of linking three kinases by covalent bonding. The scaffold-mediated assembly seems to have advantages over the covalent assembly, such as simple and facile wiring of pathways.

assembly mechanism. First, the simplicity with which synthetic scaffolds can wire the mating MAPK pathway suggests that scaffolds can promote rapid modular evolution in the face of changing environments and signaling needs. Second, scaffolds can enhance the combinatorial relationships among a limited set of signaling components and then maximize the number of specific pathways by allowing components to be shared in multiple pathways, as shown in the plasticity experiments in this study. Third, the logic gate-like behavior of scaffold-mediated assembly provides a means to control the pathway activation with rigorous accuracy. Our study showed that the modular characteristics of the synthetic scaffold assembly materialized an AND logic gate, which integrated signaling information via simple binding affinities for the three member kinases and the plasma membrane. The synthetic scaffold could not activate the mating signaling pathway when any one of these four interactions was perturbed (Fig. 6). Fourth, the synthetic scaffolds allow for the artificial control of signaling behaviors with ease. The results showed that incorporating pathway-specific phosphatases decreased the signaling amplitude, and that manipulating the binding affinity between the synthetic scaffold and the terminal kinase Fus3 could alter the signaling magnitude. These findings imply that the scaffolding mechanism allows for a facile modulation of signaling behaviors which would help to better adapt to the changing environments. During the early course of evolution, a simple tethering scaffold may have been sufficient to define a specific, though primitive, signaling pathway (*26*)

within a network of promiscuously interacting kinases. The response parameters of this pathway could then be refined through further evolution of the scaffold. In this study, we have essentially recapitulated the emergence of scaffolds during the evolution by rewiring the signaling proteins of an existing pathway using synthetic scaffolds.

The modular architecture of the rewired pathway circuit allowed us to test the levels of plasticity of the three tiers of the MAPK pathway in the synthetic scaffold platform. The tolerance of each tier to non-cognate pathway kinases was monitored when kinases in the mating MAPK pathway were replaced one at a time with a kinase from the corresponding tier of non-cognate MAPK pathways in yeast. We demonstrated that each tier of the MAPK pathway has decreasing positional plasticity from the top (MAPKKK) to the bottom tier (MAPK) of the cascade. These results may indicate the signaling demands for accommodating multiple upstream inputs at the upper tiers of pathways and for dictating signaling specificity by a terminal kinase at the bottom tier. The higher plasticity at the top tier may allow for the possibility that a new scaffold protein could be engineered or evolved to wire a signaling pathway with a novel connectivity.

Interestingly, the synthetic scaffold carrying two PDZ domains (PDZ_2^{MTD}) generated a substantial magnitude of signaling output from a three-tiered kinase cascade. As described above, this observation can be explained by either the dynamic interaction between synthetic scaffolds and

kinases or the cross-activation of kinases among different scaffold complexes. This finding is an intriguing experimental demonstration that one molecule of a scaffold protein does not have to bind to all component members simultaneously during active signaling (*40*).

Scaffold strategies have been adopted by nature in the case of pathogens or viruses manipulating the signaling responses or physiology of host cells (*37*, *38*). In our study, the co-expression of the crippled synthetic scaffold PDZ_4 in wild-type cells expressing Ste5 dramatically decreased the strength of the signaling mediated by the native scaffold Ste5, suggesting that PDZ_4 can compete against Ste5 for member kinases. The dominant negative behavior of PDZ_4 may be caused by segregation of the component kinases from Ste5 or the plasma membrane.

This study suggests that synthetic scaffolds may provide a useful means to rationally modulate or manipulate signaling pathways. The strategy is not limited to yeast but is also applicable to higher eukaryotes including mammals as shown in Fig. 15, which demonstrates that synthetic scaffold proteins could mediate prolonged ERK activation in mammalian cells. Although the modularity in the signaling networks is not as well validated as in the transcription systems, efforts have been made to synthesize or to evolve custom modular domains with novel binding specificities, which could be utilized to wire synthetic signaling cascades (*36, 45, 46*). Ultimately, such designer scaffolds composed of engineered

domains may be used to redirect the flow of signaling information for artificially controlling cellular physiology or fixing signaling malfunctions in the diseased cells.

CONCLUSION

Scientists observe a natural phenomenon and then postulate a hypothesis to explain it. They design experiments to demonstrate the hypothesis. Furthermore, they generalize the theory and apply that to anticipate what would happen in the future, for example, when they throw a ball at an angle of 60 degrees and with an initial velocity of 20 meter per second. To test a theory, they usually build up a system and restrict experimental conditions to simplify and clarify what they want to demonstrate. For instance, to show the fact that the acceleration of gravity is constant regardless of mass, physicists would drop a feather and a metal ball in a vacuum cylinder. However, biological entities are too complex to be simplified. In many cases, biologists do not have enough techniques and knowledge to make or reorganize even a subsystem of a cell which operates independently without the rest of the system, yet. This is one of reasons why biologists have designed most of their experiments in a top-down approach, which aims to gain insights into a system by breaking down the system. This is one of most effective ways to study biology, but bottom-up approach is also one of important steps toward disclosing unrevealed scientific facts and developing novel scientific insights.

In this paper, we took the synthetic approach to rebuild the subsystem of mating MAPK signaling complex, which is otherwise mediated by the

native scaffold Ste5 in yeast. We designed synthetic scaffolds with well-characterized modular interaction domains to reorganize the mating MAPK signaling pathway. We found that interaction domains in scaffolds recruited three member kinases into plasma membrane and that the scaffold-mediated protein complex generated mating signaling and physiological responses related to it. We think this does not show how the native scaffold actually functions, but rather, show how scaffolds could function in principle with minimal set of elements. The synthetic scaffold shows the possibility to operate as a signaling circuit board to integrate signaling information via simple binding affinities with rigorous accuracy. We also showed that synthetic scaffolds could be used to manipulate and engineer signaling pathway using modular characteristics of the scaffold. Furthermore, modular scaffold proteins allowed us to test the level of plasticity of the three tiers of the MAPK pathway. We demonstrated that each tier of the MAPK pathway has decreasing positional plasticity from the top (MAPKKK) tier to the bottom tier (MAPK). These findings imply that the scaffolding mechanism allows for an easy way to modulate signaling behaviors. It would help cells to meet new signaling requirements by better adapting to the changing environments. It also gives us insights into how scaffold proteins may have been emerged as simple tethering scaffolds in the early course of evolution. In addition, we also found that PDZ_2^{MTD} mediated substantial mating responses. This finding demonstrates that reactor model is not the working

mechanism of the synthetic scaffold proteins, and suggests there could be another possibilities in scaffolding mechanism.

Previous efforts to reveal facts about the mating signaling and the native scaffold Ste5 enabled us to attempt this bottom-up approach. And this study demonstrated and suggested some intriguing biological insights into the system which should not be discovered with the traditional approach. This two approaches would help each other to better understand the mechanisms of cell signaling, and the synthetic approach should allow the rational manipulation or engineering of signaling pathways.

MATERIALS AND METHODS

Cell culture, constructs and strains

Yeast cells were grown in synthetic complete (SC) media for maintaining plasmids. For galactose (2%, w/v) induction, glycerol (3%, v/v) and lactic acid (2%, w/v) were used as carbon sources instead of glucose. The results with this medium did not show noticeable differences from those with a raffinose-containing medium (2%, w/v) (Fig. 17). Table 1 shows the plasmids that were used in this study. The origin of the second PDZ domain of PSD95 is *Rattus norvegicus (30).* PDZ domains were connected with 10-peptide linkers that were 5-tandem arrays of Gly-Ser to make PDZ_n^{MTD} flexible. The MTD, which is called CTM (residues 85–115 of Snc2), originated from the Snc2 gene of *Saccharomyces cerevisiae (22).* GST or the MTD was connected to synthetic scaffolds with a 6-peptide linker that primarily consisted of Gly and Ser. The GST-PDZ_4 constructs interacted through the GST portion (Fig. 18A). The presence of GST was not essential for signaling and reduced the signal through the synthetic circuit (Fig. 18B and 18C).

The yeast strains used in this study are listed in Table 2. Plasmids and strains used in specific experiments are listed in Table 3 and Table 4, respectively. Gene knockouts and substitutions were conducted using standard gene disruption or substitution techniques.

Co-immunoprecipitation

For the preparation of lysates, cells bearing plasmids were grown to log-phase (OD_{600} = ~0.7) at 30℃ in selective media, treated with galactose (2%, w/v) for induction and further grown for 4 hours at 30℃ before harvesting. The media with cells (50 mL) were harvested, and the cells were resuspended in lysis buffer (100 mM Tris-Cl [pH 7.6], 150 mM NaCl, 0.2% (v/v) Triton X-100, 1 mM dithiothreitol [DTT], and 5 mM ethylenediaminetetraacetic acid [EDTA]) containing a protease inhibitor cocktail (Sigma) and incubated at 4℃ for 20 minutes with vigorous shaking.

To detect Fus3, Slt2, and Hog1 dual phosphorylation, two phosphatase inhibitor cocktails (Sigma) were added. After the cells were incubated, the lysates were cleared two times by centrifugation at *16,000* × *g* for 10 minutes. For immunoprecipitation (IP) and detection, the cleared lysates were mixed with 20–40 μL of anti-myc (Sigma) or anti-hemagglutinin (HA) agarose beads (Sigma) and incubated at 4℃ for 4 hours with gentle rotation. The beads were washed three times with 0.4 mL of ice-cold TST buffer (50 mM Tris-Cl [pH 7.5], 150 mM NaCl, and 0.1% (v/v) nonyl phenoxypolyethoxylethanol-40). The washed beads were resuspended in 30–50 μL of sodium dodecyl sulfate (SDS) sample buffer without DTT. The same concentrations of lysates (based on the Bradford assay), quantities of agarose beads, and amounts of SDS sample buffer were used. HA-tagged

Ste11, Ste7, Fus3, and Slt2 were detected using anti-HA antibody. PDZ_4-myc_{13} and GST-myc_{13} were detected using anti-myc antibody. Flag-tagged GST-PDZ_4 was detected using anti-Flag antibody (Sigma). Fus3 and dual-phosphorylated Fus3 were detected using anti-Fus3 antibody (Santa Cruz) and anti-phospho P44/42 antibody (Cell Signaling), respectively. Dual-phosphorylated Slt2 was detected using anti-phospho P44/42 antibody (Cell Signaling). Hog1 and dual-phosphorylated Hog1 were detected using anti-Hog1 antibody (Santa Cruz) and anti-P38 antibody (Cell Signaling), respectively. West Pico chemiluminescent substrate (Pierce) was used for detection.

Fus1-lacZ assay

β-Galactosidase assays were performed following standard protocols. The transformants were grown to log phase (OD_{600} = 0.7–0.9) at 30℃ in SC media with glycerol (3%, v/v) and lactic acid (2%, w/v) as carbon sources. At the log phase, the cells were treated with galactose (2%, w/v) for synthetic scaffolds or α-factor (10 μM) for Ste5 for 4 hours and then used for β-galactosidase assays, except in the experiments shown in Fig. 11A. In Fig. 11A, transformants were grown in SC media containing raffinose (2%, w/v) as a carbon source and treated with galactose (2%, w/v) for 5 hours. The Fus1-lacZ assays were performed in triplicate and each of the points represents the mean value ± standard deviation.

Mating assays

For mating growth assays, transformants were grown in several small rectangular forms on agar plates of SC media with glycerol (3%, v/v) and lactic acid (2%, w/v) instead of glucose, after which the transformants were mated by replica plating onto the lawn of the mating tester strain IH1793 (α-type haploid cells) on agar plates containing synthetic deficient media with galactose (2%, w/v) instead of glucose. Then, the transformants were incubated at 30℃ for 2 to 3 days (*47*).

For quantitative mating assays, the transformants were mixed with 10^7 cells of the IH1793 strain. The mixed cells were collected onto sterile filters, and the filters were placed on agar plates containing SC media with galactose (2%, w/v) instead of glucose for 8 hours at 30℃. The harvested cells on the filters were diluted and plated on selective media for either diploids or the total of plasmid-bearing cells. The mating efficiency was (**a** / α) / (**a** + (**a** / α)) (*47*).

Flow cytometry

The transformants were treated with galactose (2%, w/v) during early log-phase and analyzed using a BD FACSCalibur. The fluorescence of 10,000 cells was measured for each reading. EGFP (green) and T1 (red) were detected at excitation and emission wavelengths of 488 nm and 515–

545 nm or 564–606 nm, respectively (*48*). In all figures, the assays used to detect Fus1-EGFP or Fus-T1 were performed in triplicate. Each of the points represents the mean value ± standard deviation.

Halo assay

SH156 or RB201 transformants (2×10^6 cells) were mixed with 5 mL of SC media using glycerol (3%, v/v) and lactic acid (2%, w/v) as carbon sources and agar (0.5%, w/v). The media with cells were poured onto agar plates of SC media containing glycerol (3%, v/v) and lactic acid (2%, w/v) as carbon sources. After the top agar dried, filter discs (1/4-inch diameter) were placed on the surface, and 10 μL of either galactose (20%, w/v) or α-factor (1 mM) was applied to the discs. The plates were incubated at 30°C for 2 to 3 days. A lack of cell growth around the discs indicates inducer-dependent cell cycle arrest, which is a mating response.

ERK dual phosphorylation assay.

Plasmids containing myc-tagged PDZ4 and Flag-tagged Raf-1, Mek1, and Erk1 were transfected into 293T cells using Genefectine Reagent (Genetrone Biotech). PDZ_4 and the three kinases were detected using anti-myc antibody and anti-Flag antibody (Sigma), respectively. The transfected cells were treated with EGF (100 ng/mL) for 1 hour after overnight starvation with FBS (0.5%, v/v) and then lysed with lysis buffer (50 mM

HEPES [pH 7.4], 150 mM NaCl, 2 mM PMSF, 10 mM NaF, 1 mM aprotinin, 1 mM leupeptin, 1 mM pepstatin A, 0.1 mM Na_3VO_4, and 1 mM DTT) containing two phosphatase inhibitor cocktails (Sigma). Dual-phosphorylated ERK was detected using anti-phospho P44/42 antibody (Cell Signaling). A West Pico Chemiluminescence Kit (Pierce) was used for detection.

Figure 17.

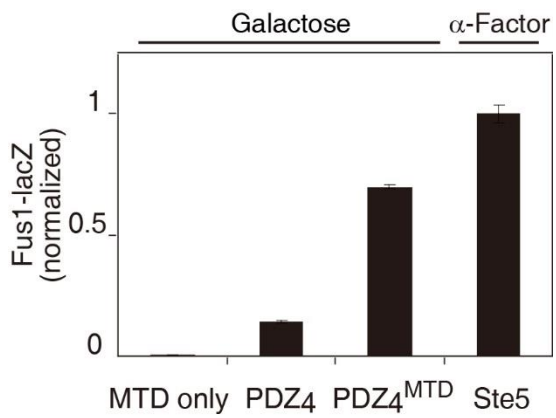
Galactose
α-Factor
Fus1-lacZ (normalized)
1
0.5
0
MTD only
PDZ4
PDZ4MTD
Ste5

Figure 17. The results with media containing raffinose (2%, w/v) as a carbon source. The results did not show a noticeable difference from the results using media containing glycerol (3%, v/v) and lactic acid (2%, w/v). Most of the experiments were performed with the media containing glycerol and lactic acid for galactose induction. The PDZ_4^{MTD}-mediated mating response with the media containing raffinose was slightly higher than that with the media containing glycerol and lactic acid. The average values and standard deviations of three experiments are shown.

Figure 18.

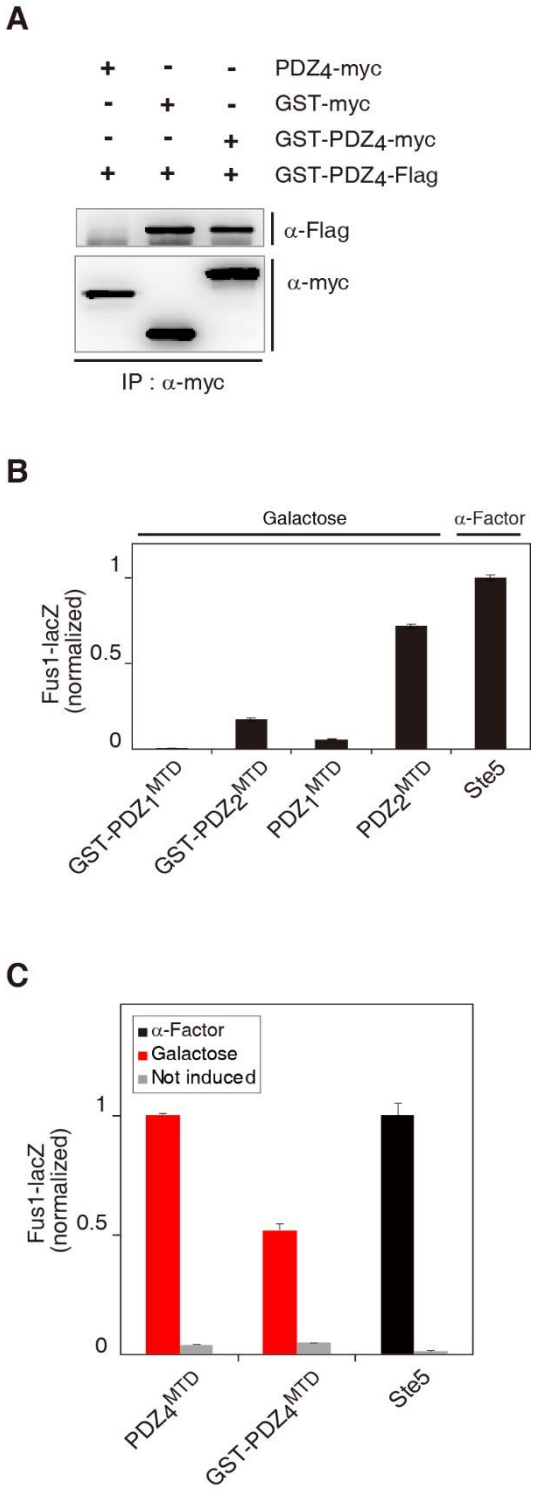
A
+ - - PDZ4-myc
- + - GST-myc
- - + GST-PDZ4-myc
+ + + GST-PDZ4-Flag
α-Flag
α-myc
IP : α-myc
B
Galactose
α-Factor
Fus1-lacZ (normalized)
1
0.5
0
GST-PDZ1MTD
GST-PDZ2MTD
PDZ1MTD
PDZ2MTD
Ste5
C
α-Factor
Galactose
Not induced
Fus1-lacZ (normalized)
1
0.5
0
PDZ4MTD
GST-PDZ4MTD
Ste5

Figure 18. Effects induced by the oligomerization of synthetic scaffolds. (A) PDZ_4 scaffolds with the GST domain tethered each other in a GST-dependent manner. (B, C) The oligomerization of the synthetic scaffolds decreased the strength of the mating response. The average value and standard deviation of three experiments are shown. This finding suggests that the oligomerization of PDZ_4^{MTD} is not necessary for PDZ-based synthetic scaffold assembly. Therefore, we did not specify the use of the GST domain in scaffold proteins in the rest of the manuscript. PDZ_4^{MTD} scaffolds without the GST domain were used in Fig. 7~13, and 15.

Table 1. Plasmids used in this study.

Plasmid	Parent vector	Promoter	Description
pSH1513	pRS314	Gal1	GST-myc_{13}
pSH1521	pRS314	Gal1	GST-PDZ1-myc_{13}
pSH1522	pRS314	Gal1	GST-PDZ2-myc_{13}
pSH1523	pRS314	Gal1	GST-PDZ3-myc_{13}
pSH1529	pRS314	Gal1	GST-PDZ4-myc_{13}
pSH1530	pRS314	Gal1	GST-PDZ5-myc_{13}
pSH1545	pRS314	Gal1	GST-PDZ6-myc_{13}
pSH1546	pRS314	Gal1	GST-PDZ7-myc_{13}
pSH1534	pRS314	Gal1	GST-MTD
pSH1548	pRS314	Gal1	GST-PDZ1-MTD
pSH1549	pRS314	Gal1	GST-PDZ2-MTD
pSH1535	pRS314	Gal1	GST-PDZ3-MTD
pSH1536	pRS314	Gal1	GST-PDZ4-MTD
pSH1537	pRS314	Gal1	GST-PDZ5-MTD
pSH1550	pRS314	Gal1	GST-PDZ6-MTD
pSH1551	pRS314	Gal1	GST-PDZ7-MTD
pSH1664	pRS314	Gal1	EGFP-PDZ4-myc_{13}
pSH1666	pRS314	Gal1	EGFP-PDZ4-MTD
pSH1557	pRS314	Gal1	PDZ4-myc_{13}
pSH1788	pRS314	Gal1	PDZ1-MTD
pSH1613	pRS314	Gal1	PDZ2-MTD
pSH1558	pRS314	Gal1	PDZ4-MTD
pSH1778	pRS316	Gal1	GST-PDZ4-$Flag_3$
pSH1554	pRS314	Ste5	Ste5
pSH1493	pRS314	Gal1	Ste5-EGFP
pSH1372	pRS315	Ste5	Ste5
pSH1365	pRS316	Gal1	HA3-Ste11-SIESDV
pSH1525	pRS316	Gal1	HA3-Ste7-SIESDV
pSH1531	pRS313	Gal1	HA3-Ste7-SIESDV
pSH1106	pRS316	Gal1	HA3-Fus3-SIESDV
pSH1532	pRS315	Gal1	HA3-Fus3-SIESDV
pSH1254	pRS316	Gal1	HA3-Ste11
pSH1553	pRS313	Gal1	HA3-Ste7
pSH1533	pRS315	Gal1	HA3-Fus3

pSH1312	pRS316	Ste11	Ste11-SIESDV
pSH1559	pRS313	Ste7	Ste7-SIESDV
pSH1560	pRS315	Fus3	Fus3-SIESDV
pSH1577	pRS316	Ste11	Ste11
pSH1578	pRS313	Ste7	Ste7
pSH1561	pRS315	Fus3	Fus3
pSH1657	pRS315	Fus3	HA3-Fus3-SIESDV
pSH1658	pRS315	Fus3	HA3-Fus3
pSH1863	pRS313	Gal1	HA3-Msg5-SIESDV
pSH1865	pRS313	Gal1	HA3-Ptp3-SIESDV
pSH1631	pRS316	Fus1	EGFP
pSH1815	pRS316	Fus1	$EGFP^{PEST}$
pSH1869	pRS316	Fus1	T1(RFP)
pSH1667	pRS316	Gal1	HA3-Ssk22-SIESDV
pSH1668	pRS316	Gal1	HA3-Ssk22
pSH1811	pRS313	Gal1	HA3-Pbs2(360-633)
pSH1812	pRS313	Gal1	HA3-Pbs2(360-633)-GSx5-SIESDV
pSH2379	pRS313	Ste7	HA3-Pbs2(360-633)-GSx5-SIESDV
pSH2380	pRS313	Ste7	HA3-Pbs2(360-633)
pSH2381	pRS313	Ste7	HA3-Pbs2(1-67)-Pbs2(360-633)-GSx5-SIESDV
pSH2382	pRS313	Ste7	HA3-Pbs2(1-67)-Pbs2(360-633)
pSH1653	pRS315	Gal1	HA3-Hog1-SIESDV
pSH1654	pRS315	Gal1	HA3-Hog1
pSH1655	pRS315	Hog1	HA3-Hog1-SIESDV
pSH1656	pRS315	Hog1	HA3-Hog1
pSH2349	pRS316	Gal1	HA3-Bck1-SIESDV
pSH2350	pRS316	Gal1	HA3-Bck1
pSH1858	pRS313	Ste7	HA3-Mkk1-SIESDV
pSH1859	pRS313	Ste7	HA3-Mkk1
pSH1860	pRS313	Ste7	HA3-Mkk2-SIESDV
pSH1861	pRS313	Ste7	HA3-Mkk2
pSH2353	pRS315	Gal1	HA3-Slt2-SIESDV
pSH2354	pRS315	Gal1	HA3-Slt2
pSH2657	pRS315	Fus3	HA3-Fus3-VKEALV
pSH2658	pRS315	Fus3	HA3-Fus3-VKESLA

pSH2076	pRS315	Ste7	Ste7
pSH2628	pRS315	Ste7	Ste7-SIESDV
pSH2630	pRS315	Ste7	$Ste7^{ND1,ND2}$-SIESDV
pSH1994		CMV	
pSH2326		CMV	PDZ4-MTD-Myc
pSH2327		CMV	Flagx3-Raf-1(human)-GSGS -SIESDV
pSH2329		CMV	Flagx3-MEK1(human)-GSGS -SIESDV
pSH2335		CMV	Flagx3-ERK1(human)-GSGS -SIESDV
pRS313			
pRS314			
pRS315			
pRS316			

pRS313 is a low-copy yeast vector (*CEN/ARS*, *HIS3*)

pRS314 is a low-copy yeast vector (*CEN/ARS*, *TRP1*)

pRS315 is a low-copy yeast vector (*CEN/ARS*, *LEU2*)

pRS316 is a low-copy yeast vector (*CEN/ARS*,*URA3*)

SIESDV, Ser-Ile-Glu-Ser-Asp-Val (Binding target peptide of the second PDZ domain of PSD95)

Table 2. Yeast strains used in this study.

Strain	Description
RB201	*MAT***a**, *mfa2::pFus1-LacZ, ste5::Kan^R, his3, trp1, leu2, ura3*
SH156	*MAT***a**, *ste11::Ste11-SIESDV, ste7::Ste7-SIESDV, mfa2::pFus1-LacZ, ste5::Kan^R, his3, trp1, leu2, ura3*
SH165	*MAT***a**, *ste11::Ste11-SIESDV, ste7::Ste7-SIESDV, pbs2::His3MX6, mfa2::pFus1-LacZ, ste5::Kan^R, his3, trp1, leu2, ura3*
SH166	*MAT***a**, *ste20::CaUra3, ste11::Ste11-SIESDV, ste7::Ste7-SIESDV, mfa2::pFus1-LacZ, ste5::Kan^R, his3, trp1, leu2, ura3*
SH168	*MAT***a**, *ste11::Ste11-SIESDV, ste7::Ste7-SIESDV, fus3::Fus3-SIESDV, mfa2::pFus1-LacZ, ste5::Kan^R, his3, trp1, leu2, ura3*
SH193	*MAT***a**, *ste11::Ste11-SIESDV, ste7::His5(S.pombe), fus3::Fus3-SIESDV, mfa2::pFus1-LacZ, ste5::Kan^R, his3, trp1, leu2, ura3*
IH1793	*MATα, lys1*

Table 3. Plasmids used in specific experiments.

Figure	Plasmids used
Figure 2A	pSH1254, pSH1365, pSH1513, pSH1529, pSH1531, pSH1532, pSH1533, pSH1553
Figure 2B	pSH1493, pSH1560, pSH1561, pSH1664, pSH1666
Figure 3A	pSH1536, pSH1554, pSH1560
Figure 3B	pSH1536, pSH1554, pSH1657, pSH1658
Figure 3C	pSH1534, pSH1535, pSH1536, pSH1537, pSH1548, pSH1549, pSH1550, pSH1551, pSH1560, pSH1631
Figure 4A	pSH1534, pSH1535, pSH1536, pSH1548, pSH1549, pSH1554, pSH1560
Figure 4B	pSH1529, pSH1534, pSH1536, pSH1554, pSH1558, pSH1560, pSH1561
Figure 5A	pSH1312, pSH1534, pSH1536, pSH1559, pSH1560, pSH1561, pSH1577, pSH1578
Figure 5B	pSH1534, pSH1536, pSH1554, pSH1560, pSH1561, pSH1613
Figure 5C	pSH1534, pSH1536, pSH1554, pSH1560, pSH1561
Figure 7A	pSH1554, pSH1558, pSH1560, pSH1561, pSH1815
Figure 7B	pSH1536
Figure 8A	pRS313, pSH1558, pSH1560, pSH1631, pSH1863, pSH1865
Figure 8B	pSH1558, pSH1657, pSH1658, pSH2657, pSH2658
Figure 8C	pSH1558, pSH1657, pSH1658, pSH2657, pSH2658
Figure 9	pRS313, pRS314, pSH1372, pSH1557, pSH1631
Figure 11A	pSH1365, pSH1531, pSH1532, pSH1534, pSH1558, pSH1667, pSH1668
Figure 11B	pSH1312, pSH1534, pSH1558, pSH1559, pSH1560, pSH2379, pSH2380
Figure 11C	pRS314, pSH1558, pSH1655, pSH1656
Figure 12A	pSH1365, pSH1365, pSH1531, pSH1532, pSH1534, pSH1558, pSH2349, pSH2350
Figure 12B	pSH1312, pSH1534, pSH1558, pSH1559, pSH1560, pSH1858, pSH1859, pSH1860, pSH1861

Figure 12C	pSH1534, pSH1558, pSH1657, pSH2351, pSH2352
Figure 13	pSH1558, pSH2076, pSH2628, pSH2630
Figure 15	pSH2327, pSH2329, pSH2335, pSH2326, pSH1994
Figure 17	pSH1529, pSH1534, pSH1536, pSH1554, pSH1560, pSH1561
Figure 18A	pSH1513, pSH1529, pSH1557, pSH1778
Figure 18B	pSH1548, pSH1549, pSH1554, pSH1560, pSH1561, pSH1613, pSH1788
Figure 18C	pSH1536, pSH1554, pSH1558, pSH1560

Table 4. Yeast strains used in specific experiments.

Figure	Strains used		
Figure 2A	RB201		
Figure 2B	SH156	RB201	
Figure 3A	SH156	RB201	
Figure 3B	SH156	RB201	
Figure 3C	SH156		
Figure 4A	SH156		
Figure 4B	SH156	RB201	
Figure 5A	RB201		
Figure 5B	SH156	IH1793	
Figure 5C	SH156	RB201	SH166
Figure 7A	SH156		
Figure 7B	SH168		
Figure 8A	SH156		
Figure 8B	SH156		
Figure 8C	SH156		
Figure 9	SH168		
Figure 11A	RB201		
Figure 11B	RB201		
Figure 11C	SH165	RB201	
Figure 12A	RB201		
Figure 12B	RB201		
Figure 12C	SH156		
Figure 13	SH193		
Figure 17	SH156	RB201	
Figure 18A	SH156		
Figure 18B	SH156	RB201	
Figure 18C	SH156	RB201	

REFERENCES

1. M. B. Elowitz, S. Leibler, A synthetic oscillatory network of transcriptional regulators. *Nature* **403**, 335-338 (2000).
2. T. S. Moon, C. Lou, A. Tamsir, B. C. Stanton, C. A. Voigt, Genetic programs constructed from layered logic gates in single cells. *Nature* **491**, 249-253 (2012).
3. F. Posas, H. Saito, Osmotic activation of the HOG MAPK pathway via Ste11p MAPKKK: scaffold role of Pbs2p MAPKK. *Science* **276**, 1702-1705 (1997).
4. T. Pawson, J. D. Scott, Signaling through scaffold, anchoring, and adaptor proteins. *Science* **278**, 2075-2080 (1997).
5. W. Kolch, Coordinating ERK/MAPK signalling through scaffolds and inhibitors. *Nature reviews. Molecular cell biology* **6**, 827-837 (2005).
6. J. G. Zalatan, S. M. Coyle, S. Rajan, S. S. Sidhu, W. A. Lim, Conformational control of the Ste5 scaffold protein insulates against MAP kinase misactivation. *Science* **337**, 1218-1222 (2012).
7. S. C. Strickfaden, M. J. Winters, G. Ben-Ari, R. E. Lamson, M. Tyers, P. M. Pryciak, A mechanism for cell-cycle regulation of MAP kinase signaling in a yeast differentiation pathway. *Cell* **128**, 519-531 (2007).

8. A. Zeke, M. Lukacs, W. A. Lim, A. Remenyi, Scaffolds: interaction platforms for cellular signalling circuits. *Trends in cell biology* **19**, 364-374 (2009).

9. W. A. Lim, Designing customized cell signalling circuits. *Nat Rev Mol Cell Bio* **11**, 393-403 (2010).

10. C. J. Bashor, N. C. Helman, S. Yan, W. A. Lim, Using engineered scaffold interactions to reshape MAP kinase pathway signaling dynamics. *Science* **319**, 1539-1543 (2008).

11. J. E. Ferrell, Jr., What do scaffold proteins really do? *Sci STKE* **2000**, pe1 (2000).

12. M. J. Winters, R. E. Lamson, H. Nakanishi, A. M. Neiman, P. M. Pryciak, A membrane binding domain in the ste5 scaffold synergizes with gbetagamma binding to control localization and signaling in pheromone response. *Mol Cell* **20**, 21-32 (2005).

13. K. Y. Choi, B. Satterberg, D. M. Lyons, E. A. Elion, Ste5 tethers multiple protein kinases in the MAP kinase cascade required for mating in S. cerevisiae. *Cell* **78**, 499-512 (1994).

14. C. Inouye, N. Dhillon, J. Thorner, Ste5 RING-H2 domain: role in Ste4-promoted oligomerization for yeast pheromone signaling. *Science* **278**, 103-106 (1997).

15. S. K. Mahanty, Y. Wang, F. W. Farley, E. A. Elion, Nuclear shuttling of yeast scaffold Ste5 is required for its recruitment to the plasma membrane and activation of the mating MAPK cascade. *Cell* **98**,

501-512 (1999).

16. L. S. Garrenton, S. L. Young, J. Thorner, Function of the MAPK scaffold protein, Ste5, requires a cryptic PH domain. *Genes Dev* **20**, 1946-1958 (2006).

17. R. P. Bhattacharyya, A. Remenyi, M. C. Good, C. J. Bashor, A. M. Falick, W. A. Lim, The Ste5 scaffold allosterically modulates signaling output of the yeast mating pathway. *Science* **311**, 822-826 (2006).

18. M. Good, G. Tang, J. Singleton, A. Remenyi, W. A. Lim, The Ste5 scaffold directs mating signaling by catalytically unlocking the Fus3 MAP kinase for activation. *Cell* **136**, 1085-1097 (2009).

19. S. H. Park, A. Zarrinpar, W. A. Lim, Rewiring MAP kinase pathways using alternative scaffold assembly mechanisms. *Science* **299**, 1061-1064 (2003).

20. J. Moon, S. H. Park, Reassembly of JIP1 Scaffold Complex in JNK MAP Kinase Pathway Using Heterologous Protein Interactions. *PloS one* **9**, e96797 (2014).

21. J. E. Dueber, G. C. Wu, G. R. Malmirchegini, T. S. Moon, C. J. Petzold, A. V. Ullal, K. L. Prather, J. D. Keasling, Synthetic protein scaffolds provide modular control over metabolic flux. *Nat Biotechnol* **27**, 753-759 (2009).

22. P. M. Pryciak, F. A. Huntress, Membrane recruitment of the kinase cascade scaffold protein Ste5 by the Gbetagamma complex underlies

activation of the yeast pheromone response pathway. *Genes Dev* **12**, 2684-2697 (1998).

23. K. Harris, R. E. Lamson, B. Nelson, T. R. Hughes, M. J. Marton, C. J. Roberts, C. Boone, P. M. Pryciak, Role of scaffolds in MAP kinase pathway specificity revealed by custom design of pathway-dedicated signaling proteins. *Curr Biol* **11**, 1815-1824 (2001).

24. W. Cho, Building signaling complexes at the membrane. *Sci STKE* **2006**, pe7 (2006).

25. M. Ptashne, A. Gann, Imposing specificity by localization: mechanism and evolvability. *Curr Biol* **8**, R897 (1998).

26. S. M. Coyle, J. Flores, W. A. Lim, Exploitation of latent allostery enables the evolution of new modes of MAP kinase regulation. *Cell* **154**, 875-887 (2013).

27. R. P. Bhattacharyya, A. Remenyi, B. J. Yeh, W. A. Lim, Domains, motifs, and scaffolds: the role of modular interactions in the evolution and wiring of cell signaling circuits. *Annu Rev Biochem* **75**, 655-680 (2006).

28. D. A. Drubin, J. C. Way, P. A. Silver, Designing biological systems. *Genes Dev* **21**, 242-254 (2007).

29. E. C. O'Shaughnessy, S. Palani, J. J. Collins, C. A. Sarkar, Tunable signal processing in synthetic MAP kinase cascades. *Cell* **144**, 119-131 (2011).

30. B. Z. Harris, B. J. Hillier, W. A. Lim, Energetic determinants of

internal motif recognition by PDZ domains. *Biochemistry* **40**, 5921-5930 (2001).

31. C. N. Chi, A. Bach, M. Gottschalk, A. S. Kristensen, K. Stromgaard, P. Jemth, Deciphering the kinetic binding mechanism of dimeric ligands using a potent plasma-stable dimeric inhibitor of postsynaptic density protein-95 as an example. *The Journal of biological chemistry* **285**, 28252-28260 (2010).

32. F. Drogen, S. M. O'Rourke, V. M. Stucke, M. Jaquenoud, A. M. Neiman, M. Peter, Phosphorylation of the MEKK Ste11p by the PAK-like kinase Ste20p is required for MAP kinase signaling in vivo. *Curr Biol* **10**, 630-639 (2000).

33. M. C. Good, J. G. Zalatan, W. A. Lim, Scaffold proteins: hubs for controlling the flow of cellular information. *Science* **332**, 680-686 (2011).

34. S. R. Salama, K. B. Hendricks, J. Thorner, G1 cyclin degradation: the PEST motif of yeast Cln2 is necessary, but not sufficient, for rapid protein turnover. *Molecular and cellular biology* **14**, 7953-7966 (1994).

35. X. L. Zhan, R. J. Deschenes, K. L. Guan, Differential regulation of FUS3 MAP kinase by tyrosine-specific phosphatases PTP2/PTP3 and dual-specificity phosphatase MSG5 in Saccharomyces cerevisiae. *Genes Dev* **11**, 1690-1702 (1997).

36. A. Levskaya, O. D. Weiner, W. A. Lim, C. A. Voigt, Spatiotemporal

control of cell signalling using a light-switchable protein interaction. *Nature* **461**, 997-1001 (2009).

37. A. S. Selyunin, S. E. Sutton, B. A. Weigele, L. E. Reddick, R. C. Orchard, S. M. Bresson, D. R. Tomchick, N. M. Alto, The assembly of a GTPase-kinase signalling complex by a bacterial catalytic scaffold. *Nature* **469**, 107-111 (2011).

38. X. Yu, Y. Yu, B. Liu, K. Luo, W. Kong, P. Mao, X. F. Yu, Induction of APOBEC3G ubiquitination and degradation by an HIV-1 Vif-Cul5-SCF complex. *Science* **302**, 1056-1060 (2003).

39. A. Remenyi, M. C. Good, R. P. Bhattacharyya, W. A. Lim, The role of docking interactions in mediating signaling input, output, and discrimination in the yeast MAPK network. *Mol Cell* **20**, 951-962 (2005).

40. F. Pincet, Membrane recruitment of scaffold proteins drives specific signaling. *PloS one* **2**, e977 (2007).

41. W. R. Burack, A. S. Shaw, Signal transduction: hanging on a scaffold. *Current opinion in cell biology* **12**, 211-216 (2000).

42. W. R. Whitaker, S. A. Davis, A. P. Arkin, J. E. Dueber, Engineering robust control of two-component system phosphotransfer using modular scaffolds. *Proceedings of the National Academy of Sciences of the United States of America* **109**, 18090-18095 (2012).

43. T. Rajakulendran, M. Sahmi, M. Lefrancois, F. Sicheri, M. Therrien, A dimerization-dependent mechanism drives RAF catalytic

activation. *Nature* **461**, 542-545 (2009).

44. N. Dard, M. Peter, Scaffold proteins in MAP kinase signaling: more than simple passive activating platforms. *BioEssays : news and reviews in molecular, cellular and developmental biology* **28**, 146-156 (2006).

45. S. Schneider, M. Buchert, O. Georgiev, B. Catimel, M. Halford, S. A. Stacker, T. Baechi, K. Moelling, C. M. Hovens, Mutagenesis and selection of PDZ domains that bind new protein targets. *Nat Biotechnol* **17**, 170-175 (1999).

46. J. Reina, E. Lacroix, S. D. Hobson, G. Fernandez-Ballester, V. Rybin, M. S. Schwab, L. Serrano, C. Gonzalez, Computer-aided design of a PDZ domain to recognize new target sequences. *Nat Struct Biol* **9**, 621-627 (2002).

47. G. F. Sprague, Jr., Assay of yeast mating reaction. *Methods in enzymology* **194**, 77-93 (1991).

48. R. E. Campbell, O. Tour, A. E. Palmer, P. A. Steinbach, G. S. Baird, D. A. Zacharias, R. Y. Tsien, A monomeric red fluorescent protein. *Proceedings of the National Academy of Sciences of the United States of America* **99**, 7877-7882 (2002).

ABSTRACT IN KOREAN

국문 초록

합성 스캐폴드 단백질을 이용한 MAPK 신호전달의 재구성과 인위적 조작

스캐폴드 단백질은 진핵 생물의 세포 신호전달에서 종종 시그널 허브로서 작용하기 때문에 세포의 신호 회로를 엔지니어링하고 조작하기 위한 매력적인 대상으로 생각되어 왔다. 이러한 전제에 대한 궁극적인 실험적 증명을 위한 시도는, 모듈 식 구조를 갖는 계획적으로 디자인된 스캐폴드를 사용해서 세포의 신호전달 경로를 재구성 할 수 있는가를 실험해보는 것이다. 이 논문에서 우리는 합성 스캐폴드를 디자인해서 효모(*Saccharomyces Cerevisiae*)의 짝짓기 MAPK 신호전달 경로를 재조직 했다. 모듈식으로 상호작용하는 domains로 구성되어있는 이 합성 스캐폴드 단백질들은 짝짓기 MAPK 신호전달 경로의 멤버인 세 개의 인산화 효소들과 복합체를 이루어 이들을 세포막(plasma membrane)으로 이동시켰고, 신호 회로의 논리 게이트처럼 기능하여 짝짓기

신호 반응을 일으킬 수 있었다. 이 모듈 식 구조의 합성 스캐폴드의 복합체 형성 방식은 인공적인 신호 행동의 조작을 가능하게 했으며, 예를 들어 스캐폴드에 의해 매개되는 신호의 강도를 조절하거나 네거티브 컨트롤을 합성 스캐폴드에 포함 시킬 수 있었다. 이러한 구조는 또 MAPK 신호전달 경로의 세 단계를 구성하는 인산화 효소들이 위에서 아래쪽으로 내려갈수록 감소하는, 서로 다른 위치적 유연성을 나타내고 있다는 사실을 증명하는데 도움을 주었고, 이러한 사실은 새로운 신호전달 경로를 만들어낼 수 있다는 가능성을 보여주고 있다. 디자인된 스캐폴드를 이용하는 이러한 합성 생물학적인 방식을 통한 연구 방식은 신호 전달 경로의 계획적인 조작이나 엔지니어링을 가능하게 하고, 또한 스캐폴드 단백질의 기능적인 메커니즘과 스캐폴드와 연계된 신호 전달 경로의 진화에 대한 깊은 통찰을 제공할 것이다.

주요어: MAPK 신호전달 경로, 합성 스캐폴드 단백질, 모듈 식 구조, 위치적 유연성, 스캐폴드와 연계된 신호전달 경로의 진화